MURDOCH UNIVERSITY

Dynamic Models for Wind Turbines

Zhongyuan Pang

2014/7/15

Supervisor: Gregory Crebbin

A report submitted to the School of Engineering and Energy, Murdoch University in partial fulfillment of the requirements for the degree of Bachelor of Engineering

ACKNOWLEDGEMENTS

I would like to take this opportunity to express my gratitude to my supervisor, Dr. Gregory Crebbin for providing me with the guidance required to undertake this thesis project. Another special thanks to Mr. Shuo Huang for the support in transfer function and PI control.

ABSTRACT

With the increase of wind power capacity, wind energy is now becoming an essential part of energy production system. High wind power penetration may increase the instability of grid due to the characteristic of wind. Fortunately, with the development of power electronics, it is possible to provide a relatively stable energy production by applying power electronics to wind turbine.

Due to the complexity of wind turbine, a generic dynamic model of wind turbine can be helpful. The objective of the work is to develop a general wind turbine models that can be used for investigations.

The report had tracked the theory of wind turbine and its development, three different kinds of wind turbine are included, which are fixed speed wind turbine, variable slip wind turbine and doubly-fed induction generator wind turbine. Fundamental working theory and a model built by Matlab was provided for each of technology.

Assessment for the models was done to prove that it has the ability to reflect the characteristic of wind turbine. Despite from that, the models were done in three phase, so it has the ability to do with load flow analysis or grid stability.

GLOSSARY

$AC - - - - - Alternative\ Current$

$Cp\ - - - - - Rotor\ Power\ coefficient$

$DC - - - - - Direct\ current$

$D\ - - - - - Damping$

$DFIG - - - - - Doubly - fed\ induction\ generator$

$f\ - - - - - Frequency$

$I - - - - -\ Current$

$J - - - - -\ Moment\ of\ Inertia$

$K - - - - -\ Stiffness$

$K_u - - - - -$ Controller gain

Matlab $- - - - -$ A software developed by MathWorks for simulation

$p\ - - - - - Number\ of\ poles$

$P - - - - -\ Active\ Power$

$PID\ - - - - - Proportional - Integral\ and\ Derivative\ controller$

$PI - - - - -\ Proportional - Integral\ controller$

$Q - - - - -\ Reactive\ Power$

$R\ - - - - - Resistance$

$R_{rotor}\ - - - - - Rotor\ Radius$

$RPM - - - - -\ Revolutions\ per\ minute$

$s\ - - - - - Slip\ of\ machine$

$SCIG\ - - - - - Squirrel\ Cage\ Induction\ Generator$

$T_u - - - - -$ Oscillation period

$v - - - - -\ Velocity\ (wind\ speed)$

V $------Voltage$

$WRIG$ $-----Wound\ Rotor\ Induction\ Generator$

$X------$ $Inductance$

λ $------Flux$

$\lambda-TSR$ $-----Tip\ speed\ ratio$

β – – – – – – Balde pitch angle

ω $-----Rotational\ Speed$

$\rho------$ Air density

Γ $------Torque$

TABLE OF CONTENT

1. INTRODUCTION

1.1 BACKGROUND

Renewable energy is now playing an important role in power generation, especially in developing countries. By the end of 2012, wind energy capacity had reached 73.5GW in China. Another 18GW will be installed in 2013 according to the National Energy Association (NEA) of China (council, 2012, p. 8). Wind power generation is such a good technology that it could have wide spread applications all around the world.

The literature available shows that a large scale wind power plant may have a significant impact on the electric power grid (Smith, 1976). So make investigation on wind turbine and their dynamic models is essential. Due to the complex structure of a wind turbine, it is unrealistic to build all the components and test them one by one. Instead it is possible to build a model to represent the characteristic of wind turbine for user to test its behavior.

Modern computer based simulation software can be used to model different components and express each component by differential and algebraic equations that describe their operating characteristics. Users could exam the characteristics of a wind turbine and the interactions between machine and grid. Using the model to simulate different conditions and make predictions in real situation can be really helpful. Matlab is a well-known and powerful programming software that will be used to develop the models used in this report.

1.2 AIMS OF PROJECT

Give the fundamental knowledge of modeling wind turbines, detail the structure and interconnection between functional blocks. Despite from that, simplification methods which can reduce simulation complexity and simulation run time is also covered.

Then dynamic wind turbine models and each functional block in the models are simulated by using Simulink. Dynamic models need to reflect the basic characteristics of wind turbine and be suitable for air turbulence assessment and stability assessment. Finally validation is performed to prove that the models are suitable to represent the characteristics of practical wind turbine.

1.3 WIND TURBINE CLASSIFICATION

Wind turbines have been classified into 4 different types:

1. Fixed-speed wind turbine
2. Variable slip wind turbine
3. Doubly-fed induction generator wind turbine
4. Full-converter wind turbine

This report will cover the first three different types of wind turbine.

1.4 SUB-SYSTEMS OF A WIND TURBINE

Wind turbines are used to harness wind energy and convert it into electricity that can be fed into the electrical power grid. Generally speaking, wind turbine can be divided into three parts: mechanical system, electrical system and control system. Each of the systems mentioned above have several sub-systems. The detailed structure of a wind turbine is given in figure 1. Different parts of the wind turbine will be explained in detail in the next section.

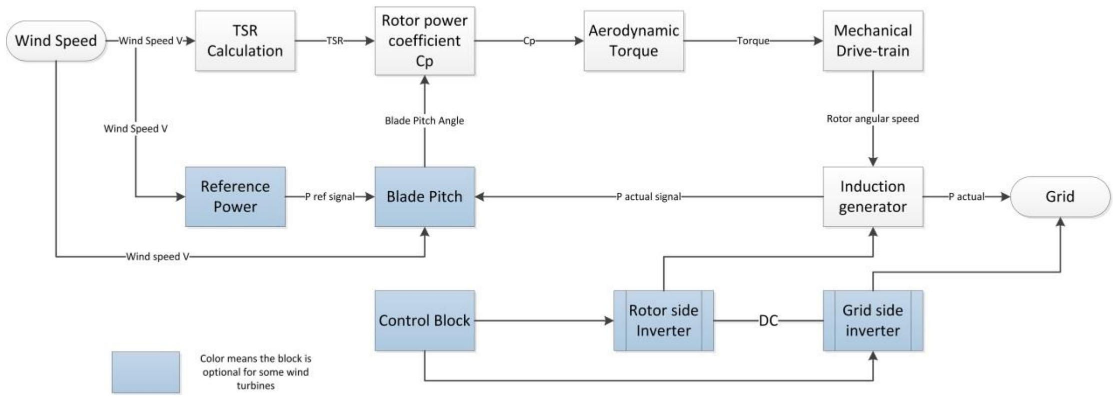

FIGURE 1 GENERIC STRUCTURE OF WIND TURBINE

2. THE SUB-SYSTEMS OF A WIND TURBINE

2.1 AERODYNAMICS

A wind turbine is a type of machine which converts wind energy into electricity. The amount of energy which is produced is based on the interaction of wind and the turbine rotor. Sometimes, wind speed may exceed the rated value, so a power limitation protection method must be applied to reduce the force acting on the wind turbine. Average power output is based on mean wind speed. This thesis focuses on the reaction of the wind turbine under steady state wind condition so turbulence is not considered.

To calculate power output of the mechanical system, tip speed ratio, rotor power coefficient and torque calculations will be introduced in this part. After that, the blade pitch control system as a protection method is described.

2.1.1 FORCE ACTING ON AIRFOIIL

Wind turbines can be classified as horizontal or vertical axis turbines based on their rotor structure. A horizontal axis wind turbine with three blades mounted together is the most popular type used in the world. Because a three blades wind turbine is the most stable and visually appealing turbine.

The shape of the blade looks like an airfoil. The two surfaces of the airfoil are different, one surface is thickened and curved while the other one is relatively flat, see figure 2. Generally speaking, two forces act on wind turbine. The lift force is perpendicular to the wind direction, while the drag force is in the same direction as the wind turbine. The lift force is the major source of wind energy.

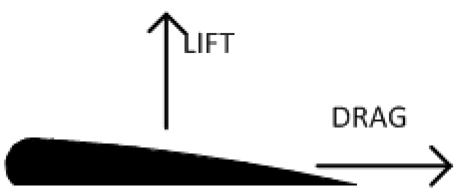

FIGURE 2 AIRFOIL

2.1.2 TIP SPEED RATIO

TSR is defined as the ratio of the blade-tip linear speed versus wind speed. "TSR can be used to find the percent of power which can be extracted by rotor" (Mohit, 2011, p. 16).

If TSR is low, wind will flow through the machine which leads to low efficiency. If TSR is too high, wind will be blocked by machine blades and cause mechanical stress.

According to the definition of tip speed ratio, TSR can be calculated as (2-1) (Mohit S. , 2011, p. 17)

$$\lambda = \frac{\omega_{rotor} * R_{rotor}}{V_{wind}} \qquad (2\text{-}1)$$

where:

ω_{rotor}=rotor angular speed [rad/s]

R_{rotor}=rotor radius [m]

V_{wind}= wind speed [m/s]

2.1.3 BETZ'S LIMIT

Betz's limit is a limitation which describes the relationship between available power in the wind and power that can be extracted by the wind turbine. The coefficient 59.3% is called Betz's coefficient (Albert, 1926). The value is the maximum energy in percent that can be harnessed by turbine.

Followed by Betz's limit, rotor power coefficient Cp is the ratio of power extracted by wind turbine and power in the wind. Cp in (Albert) is defined as (2-2)

$$C_p = \frac{Extracted\ power}{Power\ in\ the\ wind} \qquad (2\text{-}2)$$

In most of the journals, Cp is obtained by using a look up table, which is pretty simple. But this method is not accurate and is not suitable for all kinds of wind turbine. A more accurate method is to use a set of equations to describe Cp. Generic equation to calculate Cp is shown in (2-3) and (2-4) from Robert (2009).

$$C_p(\lambda,\beta) = C_1\left(\frac{C_2}{\lambda_i} - C_3\beta - C_4\right)e^{-\frac{c5}{\lambda_i}} + C_6\lambda \qquad (2\text{-}3)$$

$$\frac{1}{\lambda_i} = \frac{1}{\lambda+0.08\beta} - \frac{0.035}{\beta^3+1} \qquad (2\text{-}4)$$

Typical coefficient values for C1-C6 are:

$C_1 = 0.5176, C_2 = 116, C_3 = 0.4, C_4 = 5, C_5 = 21\ and\ C_6 = 0.0068$

Parameters can be different for different wind turbines. Detailed discussion can be found in Ragheb &M (2011).

A graph reflecting the relationship between TSR and Cp using equations (2-3) and (2-4) is plotted in figure 3. The angle in figure 3 is the angle between wind turbine and wind speed.

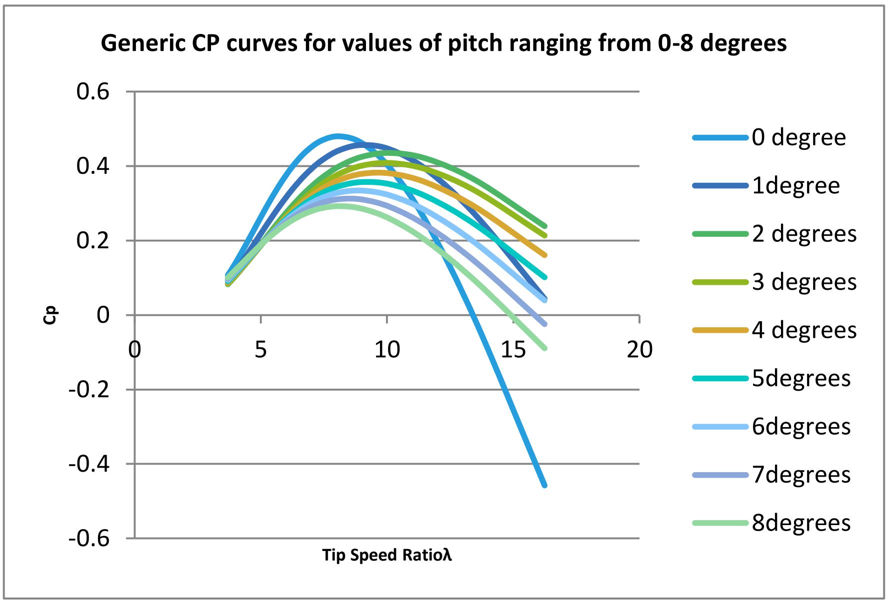

FIGURE 3 ROTOR POWER COEFFICIENT VERSUS TIP SPEED RATIO

Where the Cp in figure 3 is equal or less than 0, this implies that equation (2-3) and (2-4) are no longer valid. The line goes below zero is for completeness here. With an increase in TSR, Cp increases gradually until it reaches a maximum value, after which it decreases. Another feature of Cp is that with an increase of blade pitch angle, the coefficients decrease gradually.

2.1.4 POWER CALCULATION

Power can be calculated from the amount of wind flowing through the turbine per second. The power available in the wind is given by Royal (2014).

$$P_{wind} = \frac{1}{2}\rho A V_{wind}^3 \quad (2\text{-}5)$$

where:

ρ = air density

A =area swept by wind turbine [m^2]

V_{wind}= wind speed flow through wind turbine [m/s]

Given the rotor power coefficient Cp, the power that can be extracted from a turbine is given by equation (2-6).

$$P_{rotor} = Cp * P_{wind} = \frac{1}{2}C_p \rho A V_{wind}^3 \quad (2\text{-}6)$$

2.1.5 TORQUE CALCULATION

The torque developed by the rotor is given by equation (2-7)

$$\Gamma_{rotor} = \frac{P_{rotor}}{\omega_{rotor}} = \frac{P_{rotor} * A_{turbine}}{\omega_{rotor}} = \frac{P_{rotor} * \pi R_{Rotor}^2}{\omega_{rotor}} \quad (2\text{-}7)$$

where:

R_{rotor} = Blade Length [m]

After torque has been determined, it can be transferred into the mechanical drive-train to calculate the rotational speed of the generator shaft.

2.2 POWER CONTROL CONCEPTS

Power control is essential considering two reasons:

1. Limit power in very high winds in order to avoid damage to wind turbine.
2. Maximize the energy output.

Active and passive control methods have been developed to achieve these objectives.

2.2.1 PASSIVE STALL CONTROL

Stall regulated wind turbines have their blades designed so that when speed is higher than a certain value, the turbine blades will behave worse than expected (the point at which stall starts). The simple structure and low cost makes this popular on some turbines. The drawbacks of this application are low efficiency and the uncertainty of the behavior with the change in air density.

2.2.2 PITCH CONTROL

An active controller can be used to adjust the angle of wind turbine so that it points in the wind direction. The method could cutout the extra power so that turbine could still work at rated output and stay safe. Active controller can be expensive but accurate.

2.2.3 ACTIVE STALL CONTROL

Active stall control is a combination of the two previous methods. The stall of the blades is actively controlled by pitching the blades. “At low wind speed, turbine is controlled by pitch controller to maximize output. At high wind speed, blades go into stall and being pitched slightly into the direction opposite to that of a pitch controlled turbine” (Hansen, 2007). This combines the advantages of the previous two methods.

2.3 MECHANICAL DRIVE TRAIN

Mechanical drive train is the mechanical system for wind turbine that transfers aerodynamic torque to generator. In this thesis, two-mass model and one-mass model are introduced. “To model a wind turbine drive train, a 2-mass model is usually sufficient to represent the characteristic of drivetrain” (Okedu, 2012). First mass is the combination of components on turbine side; second mass is the combination of components on generator sides. Gear box has been assumed to be ideal in this report. There are other kinds of drive train models, comparisons between them can be found in G. Ramtharan (2006).

2.3.1 TWO-MASS MODEL

As mentioned above, two-mass model can represent the characteristics of drive train. Blades and related interactions are ignored so it can be regarded as a single mass. Gear box is assumed to be ideal so it does not have mass. Another mass is generator and its components.

Both the turbine side mass and generator side mass can be regarded as a rotational disk. A second order differential equation is used to describe its characteristic (2-8) (Mohit S. , 2011, p. 19).

$$\Gamma(t) = J\frac{d^2\theta(t)}{dt^2} + D\frac{d\theta(t)}{dt} + K\theta(t) \tag{2-8}$$

where:

J= moment of inertia

D= damping factor

K=stiffness factor

A two-mass model is shown in figure 4. Torque applied on turbine side can be transferred to generator side through gear box. From figure 4, torque applied on turbine and torque applied on gear N2 are expressed by equation (2-9) and (2-10) respectively.

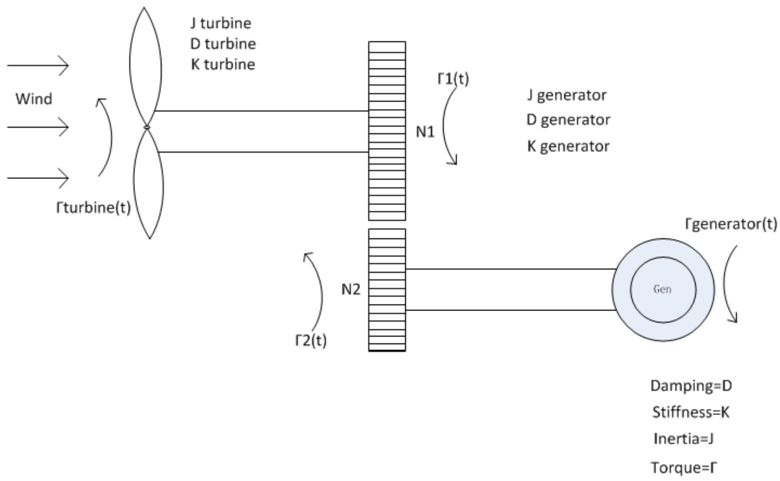

FIGURE 4 REPRESENTATION OF A TWO-MASS MODEL DRIVE TRAIN (MOHIT S. , 2011, P. 20)

$$\Gamma_{turbine}(t) = J_{turbine}\frac{d^2\theta_1(t)}{dt^2} + D_{turbine}\frac{d\theta_1(t)}{dt} + K_{turbine}\theta_1(t) + \Gamma_1(t) \tag{2-9}$$

$$\Gamma_2(t) = J_{generator}\frac{d^2\theta_2(t)}{dt^2} + D_{generator}\frac{d\theta_2(t)}{dt} + K_{generator}\theta_2(t) + \Gamma_{generator}(t) \tag{2-10}$$

For gear box, torque and gear ratio has the relationship (2-11) which is from Nathan (2004).

$$\frac{\Gamma_1}{\Gamma_2} = \frac{N_1}{N_2} \tag{2-11}$$

Based on the ratio of gear box, the relationship between torques of N_1 and N_2 can be found. After several procedures, relationship between turbine torque and generator torque is represented by equation (2-12)

$$\Gamma_{turbine}(t) = (J_{turbine} + J_{generator}\frac{N_1}{N_2}^2)\frac{d^2\theta_1(t)}{dt^2} + (D_{turbine} + D_{generator}\frac{N_1}{N_2}^2)\frac{d\theta_1(t)}{dt} + (K_{turbine} + K_{generator}\frac{N_1}{N_2}^2)\theta_1(t) + \frac{N_1}{N_2}\Gamma_{generator}(t) \qquad (2\text{-}12)$$

One thing should be noted is the parameters in equation have been transferred to one side using the gear box ratio. By solving the equation (2-12) in Simulink, shaft rotational speed can be found.

2.3.2 ONE-MASS MODEL

Models in this thesis are using one-mass model, due to the lack of damping and stiffness factors. One-mass model had neglected the effect of damping and stiffness. Inertia becomes the only thing to consider. The torque and inertia relationship had been analyzed by Florin (2004, p.27), which is given in equation (2-13).

$$\Gamma_{wind\ turbine} - \Gamma'_{generator} = J_{equivalent}\frac{d^2\theta(t)}{dt^2} \qquad (2\text{-}13)$$

Angular speed can be found by integrating (2-13) which become (2-14):

$$\frac{d\theta(t)}{dt} = \int \frac{\Gamma_{wind\ turbine} - \Gamma'_{generator}}{J_{equivalent}} \qquad (2\text{-}14)$$

2.4 GENERATOR

Many different types of generators used to be applied in wind turbines. But induction generator can be the most popular choice. Induction machine has the characteristic of low cost, robust and easy to maintain. However, during start-up, induction generator needs a leading voltage for excitation and reactive power is also required. Grid should provide those for wind turbines.

2.4.1 SQUIRREL CAGE INDUCTION GENERATOR

Squirrel cage induction generator was popular in older fixed speed wind turbines (Type I) which are cheapest and simplest. Because the shape of rotor looks like a squirrel cage, it is called squirrel cage induction generator.

During start up, current feeds into the stator windings which create a rotating magnetic field. The rotor conductors cut the rotating magnetic fields which produce a torque. Finally rotor starts to rotate. Rotor cannot rotate faster than synchronous speed if it behaves as a motor. If rotor speed is equal with synchronous speed, electrical torque will not exist, which means the rotor speed will reduce until magnetic field can cut the conductor again.

In Simulink, a squirrel cage induction machine model can be found in library. The model is employed in fixed speed wind turbine. If the simulation program does not provide a built-in model, a fifth order equation of an induction generator can be found in the appendix to model its behavior.

2.4.2 WOUND ROTOR INDUCTION GENERATOR

Wound rotor induction machine is applied in limited variable speed wind turbine (Type II) and variable speed wind turbine with partial scale frequency converters (Type III). Main difference between wound rotor machine and squirrel cage machine is the rotor winding resistance of wound rotor machine can be modified. With the control of rotor resistance, the control of generator speed can be achieved.

Equivalent circuit of a wound rotor induction machine can be found in figure 5, (Machowiski, 2008, p. 274). Iron loss is generally small so has been omitted.

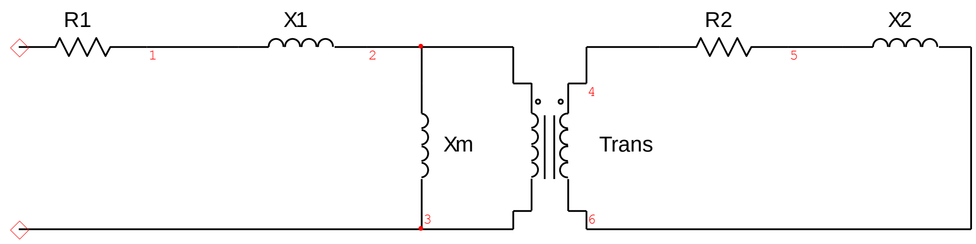

FIGURE 5 EQUIVALENT CIRCUIT OF WOUND ROTOR INDUCTION MAHCINE

In figure 5, R and X refer to the resistance and inductive reactance respectively. Subscript 1 means the value on stator side and 2 means the value on rotor side. Subscript m means the magnetizing component of the generator.

Rotor side parameters are transferred to stator side using the ideal transformer turns ratio. The circuit finally turns out as shown in the figure 6, where s represents for the slip of machine, as given by equation (2-15) from (Machowiski, 2008, p. 274).

$$Slip = \frac{\omega_{sync} - \omega_{rotor}}{\omega_{sync}} \tag{2-15}$$

where:

$\omega_{sync} = f * \frac{120}{p}$ = synchronous speed

ω_{rotor}= rotor speed

f = frequency

p = number of poles

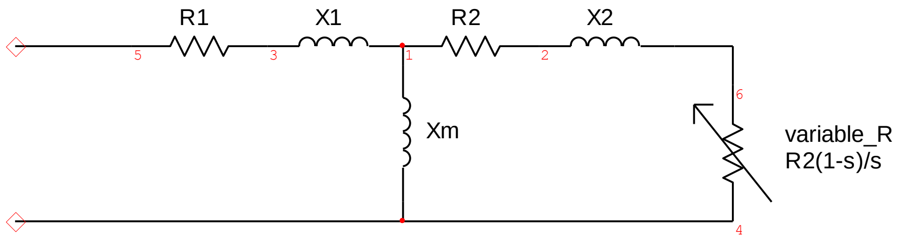

FIGURE 6 STATOR SIDE EQUIVALENT CIRCUIT OF WOUND ROTOR INDUCTION GENERATOR

Stator resistance, stator inductive reactance and magnetizing reactance in figure 6 are replaced by a Thevenin equivalent circuit. Rotor resistance and the variable resistance have the relationship (2-16), so they are combined together which is shown in figure 7.

$$\frac{R_2}{s} = R_2 + \frac{R_2(1-s)}{s} \tag{2-16}$$

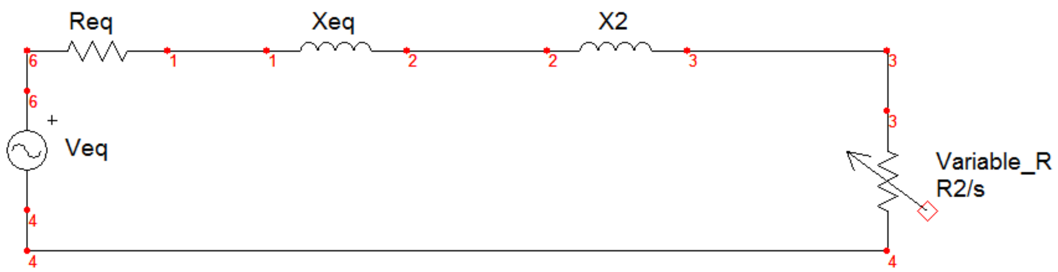

FIGURE 7 AFTER THEVENIN SIMPLIFICATION

The parameters in figure 7 is expressed as equation (2-17) and (2-18).

$$V_{eq} = \frac{jX_m}{R_1+j(X_1+X_m)} * V \quad (2\text{-}17)$$

$$R_{eq} + X_{eq} = Z_{eq} = \frac{(R_1+X_1)*X_m}{(R_1+X_1)+X_m} \quad (2\text{-}18)$$

Current flow in figure 7 can be expressed by equation (2-19).

$$I_{stator} = \frac{V}{\sqrt{(\mathrm{Req}+\frac{\mathrm{R}_2}{\mathrm{s}})^2+(\mathrm{Xeq}+\mathrm{X2})^2}} \quad (2\text{-}19)$$

One thing should be noted is the equivalent circuit represents one phase of a balanced three phase circuit. So the torque equation finally becomes equation (2-20).

$$\Gamma = 3 * \frac{\mathrm{P}}{\omega} = 3 * (\frac{\mathrm{V}}{(\mathrm{Req}+\frac{\mathrm{R}_2}{\mathrm{s}})^2+(\mathrm{Xeq}+\mathrm{X2})^2})^2 * \frac{\mathrm{R}_2}{\omega_s \mathrm{s}} \quad (2\text{-}20)$$

2.4.3 INDUCTION MACHINE WITH VARIABLE EXTERNAL ROTOR RESISTANCE

So far, external resistance is not considered in wound rotor induction generator. The reason we add an external resistance on rotor is to change of rotor resistance. A desired value of torque can be achieved at many different speeds by varying rotor resistance. Peak torque and maximal slip calculation procedures can be found in (Machowiski, 2008, p. 279).

$$S_{max} = \frac{R_2}{\sqrt{R_1^2+(X_1+X_2)^2}} \approx \frac{R_2}{X_1+X_2} \quad (2\text{-}21)$$

$$\Gamma_{max} = \frac{3}{2\omega_{sm}} \frac{V_s^2}{[R_1+\sqrt{R_1^2+(X_1+X_2)^2}]} \quad (2\text{-}22)$$

Equations expressing maximal slip and peak torque are described in (2-21) and (2-22). Equation (2-22) shows that torque will not be affected by the rotor resistance, while equation (2-21) shows that the slip at which the maximum torque occurs is determined by the rotor resistance. This means that it is possible to change slip without affecting torque of the generator.

Simply adding an external resistance on rotor side, wound rotor induction machine with external resistance is shown in figure 8.

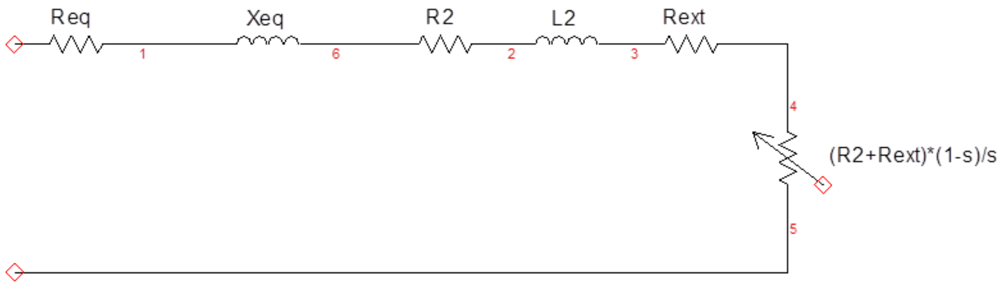

FIGURE 8 WOUND ROTOR INDUCTION MACHINE WITH EXTERNAL RESISTANCE

Equation (2-19) and (2-20) are adjusted accordingly:

$$I_{stator} = \frac{V}{\sqrt{(Req+\frac{R_2+R_{ext}}{s})^2+(Xeq+X2)^2}} \tag{2-23}$$

$$\Gamma = 3 * \frac{V^2}{(Req+\frac{R_2+R_{ext}}{s})^2+(Xeq+X2)^2} * \frac{R_2+R_{ext}}{\omega_s s} \tag{2-24}$$

By changing the external resistance, speed of the generator at which the maximum torque occurs can be changed. The torque-speed characteristic is given in figure 9.

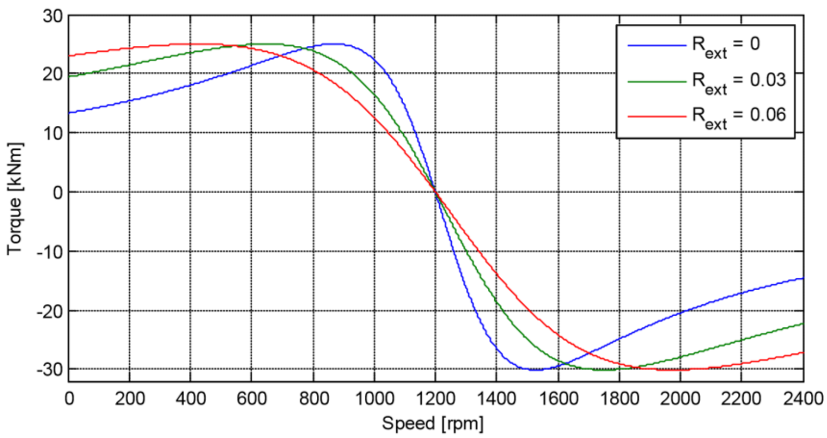

FIGURE 9 TORQUE AND SPEED CURVE OF VARIABLE RESISTANCE INDUCTION MACHINE (MOHIT, 2011)

From figure 9, maximal torque stays at different speed under different external resistances. Higher resistance gives a higher starting torque. This can be applied during the startup of motor.

If wind speed is higher than rated value, controller will change the rotational speed by changing the rotor resistance and the maximum torque stays the same. Variable slip generator wind turbine is more attractive compared with fixed-speed turbine, but in practice, speed variation range is not very attractive (only 5-10%) and efficiency of the generator is reduced due to the increase of rotor resistance.

2.4.4 DOUBLY-FED INDUCTION GENERATOR (DFIG)

The external resistance gives a small range to change and maximize the energy capture but with several drawbacks. A new method is needed which could reduce the energy loss while increasing the operation speed range of wind turbine. With the development of power electronics, generator with partial scale frequency converter achieved these aims. Despite from the advantage above, partial scale frequency converter performs reactive power compensation and the smoother grid connection. Speed operation range is also which may up to 30% of its synchronous speed" (Machowiski, 2008, p. 282).

Compared with a variable slip generator, a voltage source is applied to replay the external resistance. The voltage source is controlled by two frequency converters. These two converters are a machine side inverter and a grid side inverter. A generic structure of a DFIG can be seen in figure 10.

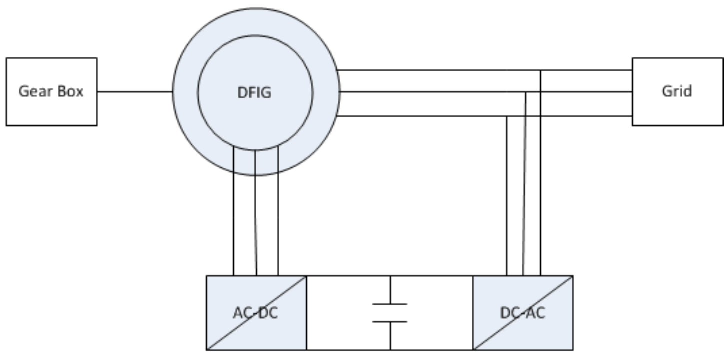

FIGURE 10 SCHEMATIC DIAGRAM OF DFIG

In variable slip generator, external resistance is used to control the voltage and current. In DFIG, the function of external resistance is replaced by a controlled voltage source. As we know the structure of a wound rotor induction machine with variable rotor resistance, if we replace the external resistance by voltage source, then stator current expression become equation (2-25).

$$\mathrm{I}_{stator} = \frac{V}{\sqrt{(\mathrm{Req}+\frac{\mathrm{R}_2+\frac{V_2}{I_{stator}}}{\mathrm{s}})^2+(\mathrm{Xeq}+\mathrm{X2})^2}} \tag{2-25}$$

Slip and torque equation are adjusted accordingly:

$$\mathrm{S} = \frac{R_2 * I_{stator} + V_2}{\sqrt{V^2-\left(X_{eq}+X_2\right)^2 * I_{stator} - R_{eq} * I_{stator}}} \tag{2-26}$$

$$\Gamma = 3 * \frac{\mathrm{V}^2}{(\mathrm{Req}+\frac{\mathrm{R}_2+\frac{V_2}{I_{stator}}}{\mathrm{s}})^2+(\mathrm{Xeq}+\mathrm{X2})^2} * \frac{\mathrm{R}_2+\frac{V_2}{I_{stator}}}{\omega_s \mathrm{s}} \tag{2-27}$$

The torque and current for a given slip can be calculated from equations above, but the equations are cumbersome and it easier to consider a range of values for $I_{stator}$and calculate the resulting torque and slip from equations respectively (O'Kelly, 1991). If current in the stator becomes 0, the slip equation (2-26) will become simplified to equation (2-28):

$$\mathrm{S} = \frac{\mathrm{V}_2}{V} \tag{2-28}$$

The slip is now controlled by the magnitude and polarity of the inserted voltage. By varying the rotor side voltage, it is possible to change slip and keep torque stable. Slip range is limited by the rating of inverter.

Rating of the inverter can be found by multiply the voltage and current flow through the controlled voltage source which is shown in (2-29).

$$S_{rating\ of\ inverter} = V_2 * I_{stator} = S * V * I_{stator} = S * S_{rating\ of\ machine} \tag{2-29}$$

As shown in equation (2-29), rating of inverter is only part of the machine rating. Such an advantage can reduce the capacity of the inverter and the capital cost of the DFIG.

Equivalent circuit of the wound rotor induction machine with variable voltage source is shown in figure 11.

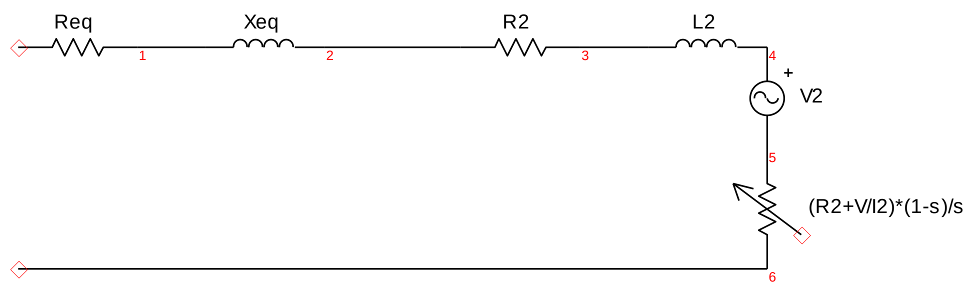

FIGURE 11 WOUND ROTOR INDUCTION MACHINE WITH VARIABLE SOURCE

To analysis the power flow of DFIG, a simplified circuit diagram of wound rotor induction machine is applied which had neglected the loss in stator resistance and iron core. The circuit is shown in figure 12. X1 is the stator resistance, R2 and X2 are rotor resistance and inductive reactance respectively.

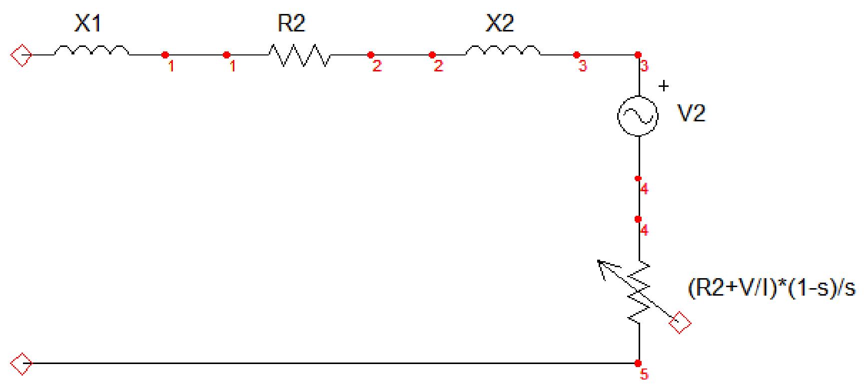

FIGURE 12WOUND ROTOR INDUCTION MACHINE

For a wound rotor induction machine, the gap power can be separated into mechanical power and power loss (2-30).

$$P_{stator} \approx P_{airgap} = P_{transfer+Loss} + P_{mech} \quad (2\text{-}30)$$

If the external voltage source is taken into consideration, equation (2-30) becomes (2-31):

$$P_{stator} \approx P_{airgap} = V2 * I_{stator} + R2 * I_{stator}{}^{2} + I_{stator} * (R2 * I_{stator} + V2) * \frac{1-s}{s} \quad (2\text{-}31)$$

$$P_{mech} = P_{airgap} * (1 - s) \quad (2\text{-}32)$$

$$P_{transfer+Loss} = P_{airgap} * s \quad (2\text{-}33)$$

If rotor resistance is small enough to be neglected, equation (2-31) finally become (2-34).

$$P_{stator} \approx P_{airgap} = V2 * I_{stator} + I_{stator} * V2 * \frac{1-s}{s} \tag{2-34}$$

From equation (2-34), generator is lossless, this is unrealistic in practice but the efficiency is much higher than type I and type II.

Due to the time constraint and the complexity of the problem, a complete partial scale frequency converter was not finished. A relatively simple method to represent the behavior of DIFG is applied.

A controlled current source is applied to achieve the function of converter. If we consider the electrical behavior of DFIG and converters: the active and reactive powers are dominated by the current regulated power converter, which means the behavior of DFIG is controlled by the converter. It behaves like a current controlled voltage source inverter which can be further simplified as a controlled current source.

Simplified models can be used to represent the electrical behavior of DFIG and accelerate the simulation speed.

2.5 CONTROL SYSTEM

Control system aims to decouple the active and reactive power and control them separately. To achieve this, stator flux oriented dq0 reference frame is applied to simplify the parameters in abc reference frame. The control of active and reactive power is achieved by using PI controller.

2.5.1 DQ0 REFERENCE FRAME

To perform conversion between dq0 reference frame and abc reference frame, Park transformation and Clarke transformation are essential. Dq0 conversion can be regarded as a combination of Park transformation and Clarke transformation. Expression of Park and Clarke Transformation are included in Appendix. The expressions of dq0 transformation and its inverse transformation are from Park (1929) which are shown in equation (2-35) and (2-36) respectively. X_{abc} *and* X_{dq0} are three phase balanced parameters and parameters in dq0 reference frame respectively.

$$Xdq0 = \sqrt{\frac{2}{3}} \begin{bmatrix} cos\theta & \cos(\theta - \frac{2\pi}{3}) & \cos(\theta + \frac{2\pi}{3}) \\ \sin(\theta) & -\sin(\theta - \frac{2\pi}{3}) & -\sin(\theta + \frac{2\pi}{3}) \\ \frac{\sqrt{2}}{2} & \frac{\sqrt{2}}{2} & \frac{\sqrt{2}}{2} \end{bmatrix} * \begin{bmatrix} X_a \\ X_b \\ X_c \end{bmatrix} \tag{2-35}$$

$$X_{abc} = \sqrt{\frac{2}{3}} \begin{bmatrix} \cos(\theta) & -\sin(\theta) & \frac{\sqrt{2}}{2} \\ \cos(\theta - \frac{2\pi}{3}) & -\sin(\theta - \frac{2\pi}{3}) & \frac{\sqrt{2}}{2} \\ \cos(\theta + \frac{2\pi}{3}) & -\sin(\theta + \frac{2\pi}{3}) & \frac{\sqrt{2}}{2} \end{bmatrix} * X_{dq0} \tag{2-36}$$

2.5.2 DECOUPLE FOR ACTIVE AND REACTIVE POWER

With dq0 transformation, the model of wound rotor induction machine can be expressed in dq0 reference frame. The detailed transformation procedure is shown in Appendix. Principle and method for decouple of active and reactive power is explained here. The procedure follows Mohit (2011).

Current in stator will produce a three phase balanced magnetic field which has a fixed magnitude and rotating at constant speed. Simply transfer the magnetic field from abc reference frame to dq0 reference frame. Let direction of d-axis be the same as the direction of the sum of flux in abc reference frame.

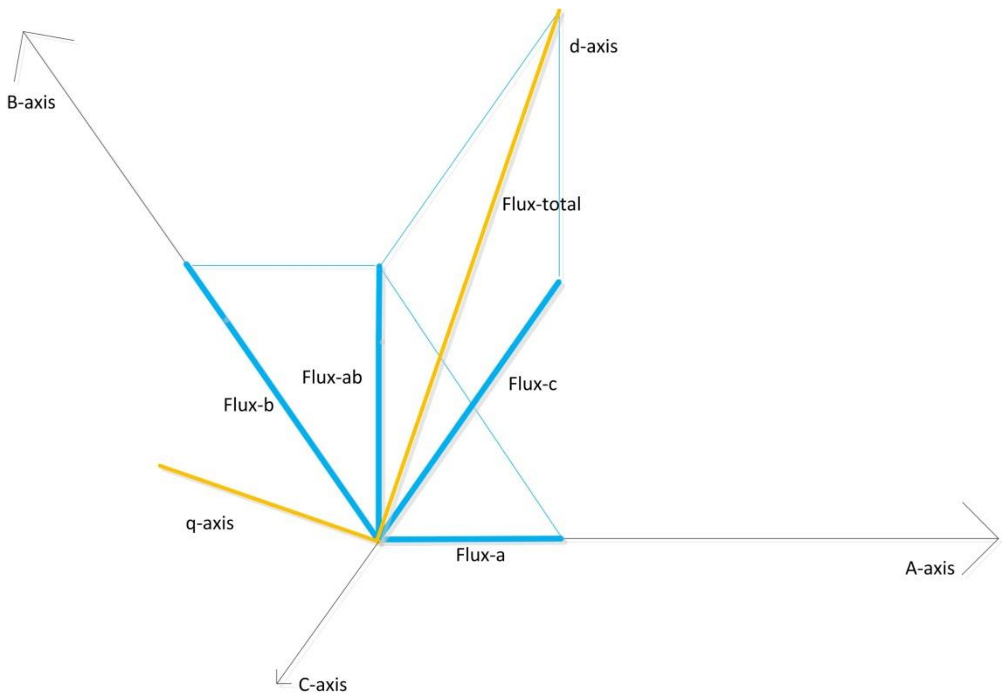

FIGURE 13 FLUX TRANSFORMATION FROM ABC TO DQ0 REFERENCE FRAME

Since the direction of flux total is the same as the direction of d-axis and q-axis is perpendicular to d-axis, so no flux locates on it. Flux can be expressed by a function of stator current and rotor current as shown in equation (2-37) and (2-38).

$$\lambda_{qs} = 0 = (L_{ls} + L_m)i_{qs} + L_m i'_{qr} \tag{2-37}$$

$$\lambda_{ds} = (L_{ls} + L_m)i_{ds} + L_m i'_{dr} \tag{2-38}$$

Rearrange equation (2-37) and (2-38) stator currents equations are shown in (2-39), (2-40).

$$i_{qs} = (-\frac{L_m}{L_{ls}+L_m})i'_{qr} \tag{2-39}$$

$$i_{ds} = (\frac{\lambda_{ds}-L_m i'_{dr}}{L_{ls}+L_m}) \tag{2-40}$$

Since the stator resistance is ignored, stator voltage can be expressed by:

$$V_{qs} = \omega\lambda_{ds} = \omega\lambda_{total} \tag{2-41}$$

$$V_{ds} = 0 \tag{2-42}$$

Under dq0 reference frame, real and reactive power are expressed by (2-43) and (2-44).

$$P_s = \frac{3}{2}\left(V_{ds}i_{ds} + V_{qs}i_{qs}\right) \tag{2-43}$$

$$Q_s = \frac{3}{2}(V_{ds}i_{qs} - V_{qs}i_{ds}) \tag{2-44}$$

If the parameters in equation (2-43) and (2-44) are substituted by equations from (2-39) to (2-42). Active and reactive power can be expressed by (2-45) and (2-46). From equation (2-45) active power is related with q-axis rotor current and from equation (2-46) reactive power is related with d-axis rotor current. Despite from that, P and Q do not have an influence on each other.

$$P_s = -\frac{3}{2}\omega\lambda_{ds}\frac{L_m}{L_{ls}+L_m}i'_{qr} \tag{2-45}$$

$$Q_s = -\frac{3}{2}\omega\lambda_{ds}\frac{\lambda_{ds}-L_m i'_{dr}}{L_{ls}+L_m} \tag{2-46}$$

From equation (2-45) and (2-46) we can draw the conclusion that: by varying rotor current, active and reactive power can be controlled independently. This means the active and reactive powers are decoupled.

2.5.3 FLUX CALCULATION

As mentioned in section 2.5.2, dq0 frame is stator flux oriented. The direction of stator flux can be essential. Flux calculation method can be different for different type of generator and its size. Detailed flux calculation method and simplification has been introduced in B.Hopfensperger (2000).

Flux angle calculation in this thesis is based on the assumption that rotor resistance can be small enough to be ignored compared with inductance so the stator voltage can be expressed by equation (2-47):

$$V_{abc} = \frac{d\lambda_{abc}}{dt} \tag{2-47}$$

So the stator flux can be calculated by integrating voltage (2-48).

$$\lambda_{abc} = \int V_{abc} * dt \tag{2-48}$$

Then three phase parameter is transformed to α, β reference frame by using Clarke transformation. By using Cartesian to polar transformation, the magnitude and flux angle of stator flux can be found.

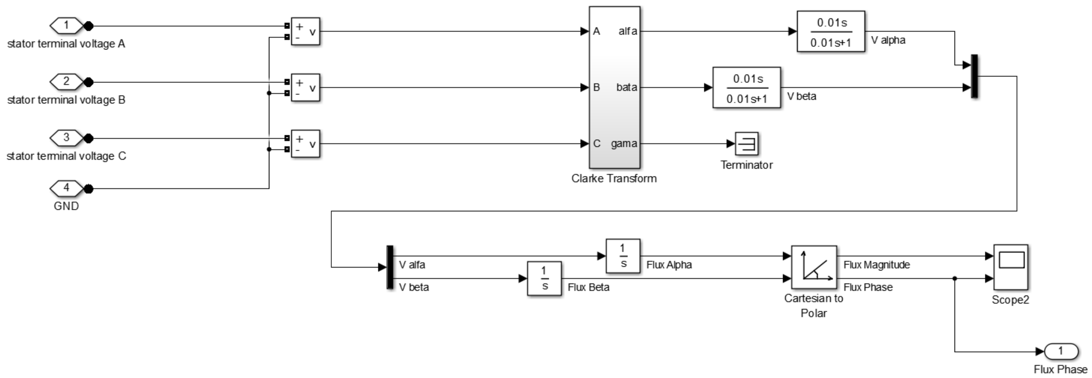

FIGURE 14 FLUX CALCULATION BLOCKS IN SIMULINK

Figure 14 represents the calculation procedures for stator flux in Simulink. Simulation results are given in figure 15. The article of W.C. Duesterhoeft (1951) had stated that the A-phase parameter should be in phase with alpha axis parameters. As shown on the left of figure 15, voltage waveform of phase A ($V_{phase\ A}$) is in phase with voltage waveforms of alpha axis (V_{alpha}). So the Clarke transformation is proved to be correct.

Right hand side of figure 15 shows that the flux magnitude and flux angle. The magnitude of flux is fixed at constant and the flux angle is keep changing from π to − π .

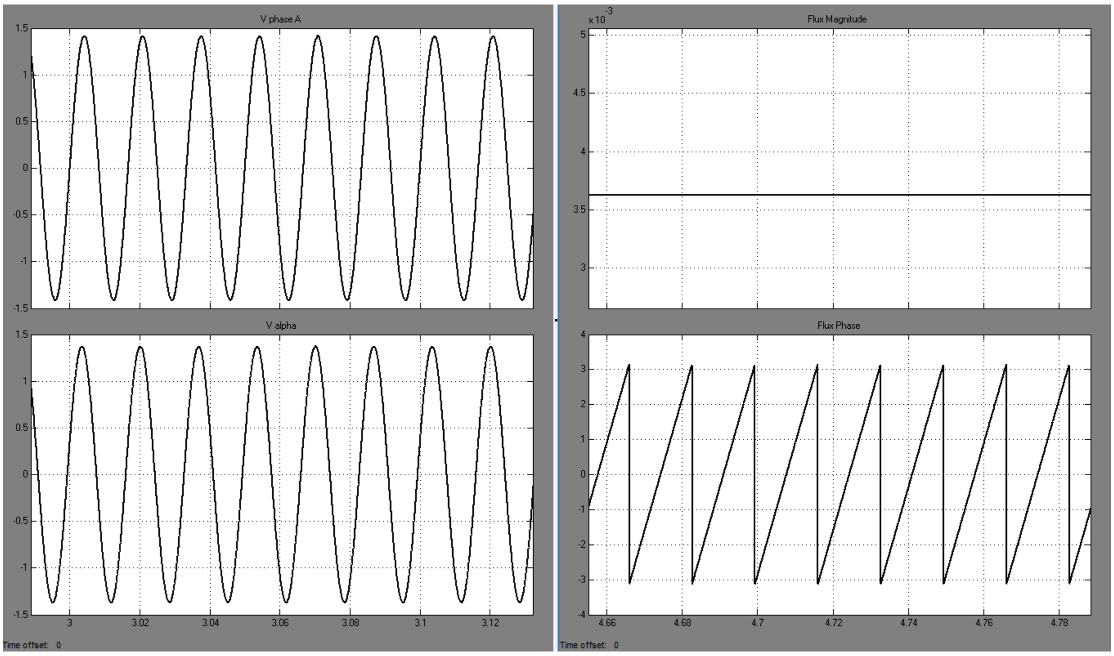

FIGURE 15 FLUX CALCULATION

2.5.4 PI CONTROLLER

PI controller is applied to control the process of wind turbine. The working theory is to minimize the difference between output and input values. A general PI controller diagram can be seen in figure 16.

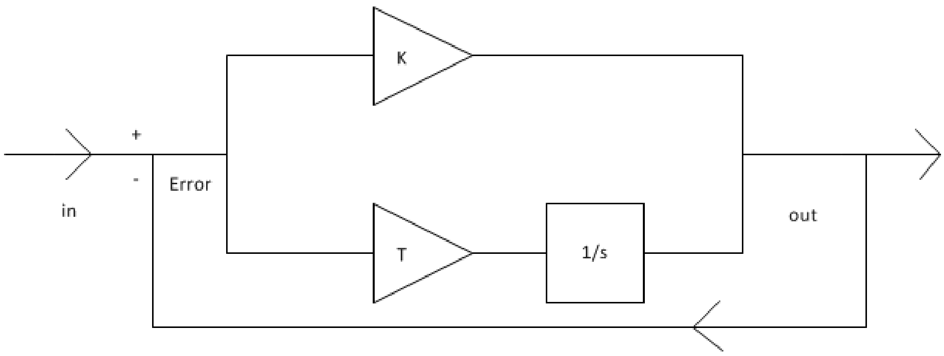

FIGURE 16 SCHEMATIC DIAGRAM OF A PI CONTROLLER (WIKI, 2014)

PI controller will reduce oscillation and steady state error compared with P controller and on and off controller, but the reaction speed can be slow, so it is often used in industrial process where the speed of response is not important (Prof. Zoran Vukic, 2002) . The response speed of a wind turbine can be slow so PI controller is sufficient for it.

To make PI controller works properly, tuning parameters are important. Ziegler-Nichols method is applied to tune the parameters which is fast and does not need complex calculation procedure compared with other methods.

For a closed loop system with proportional controller connected. Increase the parameters gradually until the system reach steady state oscillation. The oscillation should be in constant frequency and amplitude. Note down the oscillation period T_u and the controller gain K_u. Finally use table 1 to find the tuning recommendation for the PI controller.

TABLE 1 ZIEGLER-NICHOLS METHOD TUNING RECOMMENDATION (PROF. ZORAN VUKIC, 2002)

Ziegler-Nichols method tuning recommendation			
Controller Type	P	I	D
PI controller	$0.45K_u$	$0.833T_u$	N/A

3. WIND TURBINE DYNAMIC MODELS

Three different wind turbine simulation models are assembled in this part. Each functional blocks and the key issue during simulation are described. Then different validations are given to prove that the system is acceptable.

The Models are built in Simulink/Matlab. Parameters for different wind turbines are shown in Appendix.

3.1 FIXED SPEED WIND TURBINE

Figure 17 shows the complete schematic diagram of fixed-speed wind turbine implemented in Simulink. Detailed calculation procedure and working process is shown.

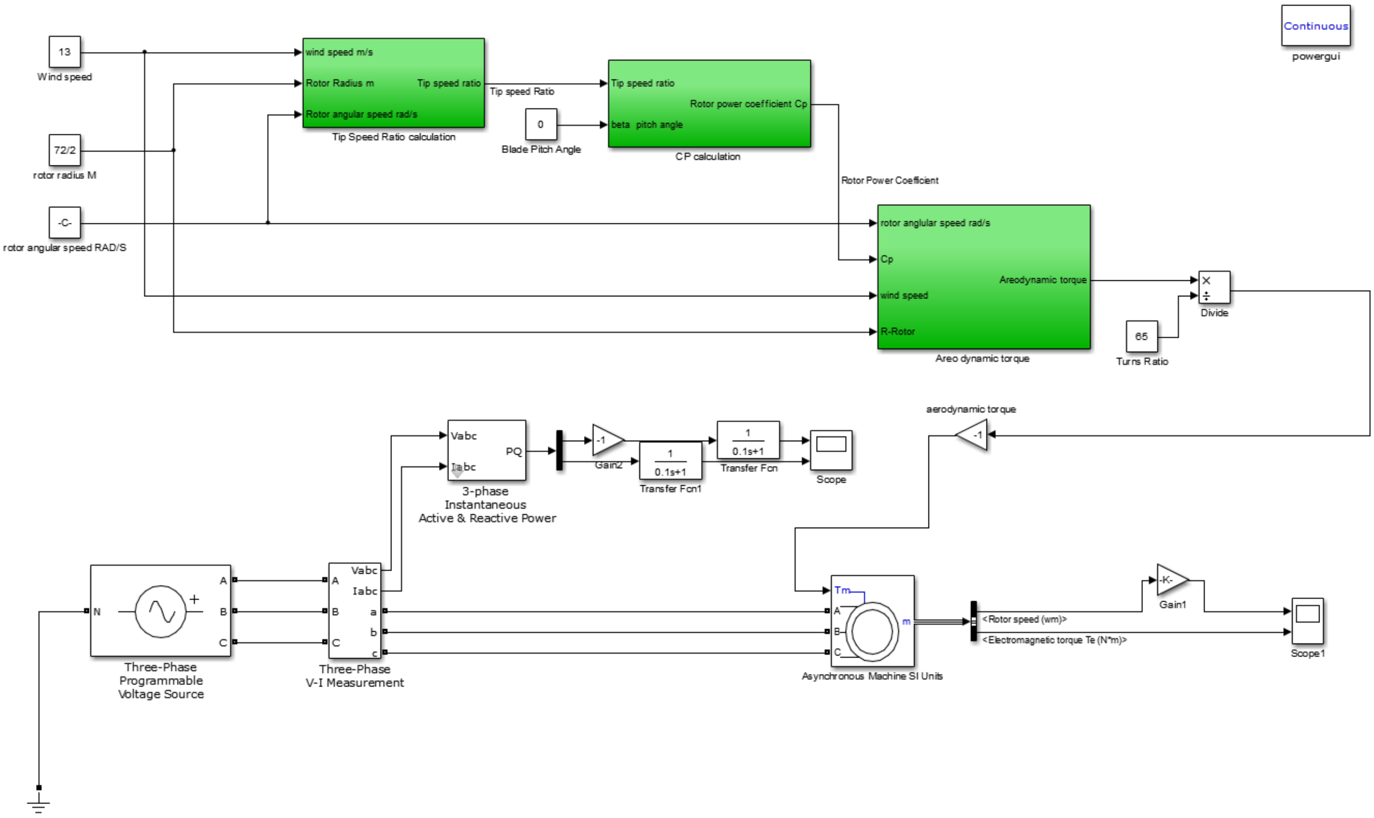

FIGURE 17 SCHEMATIC DIAGRAM FOR FIXED-SPEED WIND TURBINE

There are several points should be noted about this model. The model use passive stall control for power control, so the blade pitch angle is 0. Three-phase voltage source is implemented as an ideal grid for wind turbine. The aerodynamic torque should be negative so as to make SCIG behaves as a generator.

3.2 FIXED SPEED WIND TURBINE VALIDATION

3.2.1 POWER CURVE

Power curve for fixed speed wind turbine is shown in figure 18. Trend of the power curve is similar to the characteristic of wind turbine in real world. Passive stall effect come into existence after 15m/s which reduce the output power until turbine cut out at 20m/s.

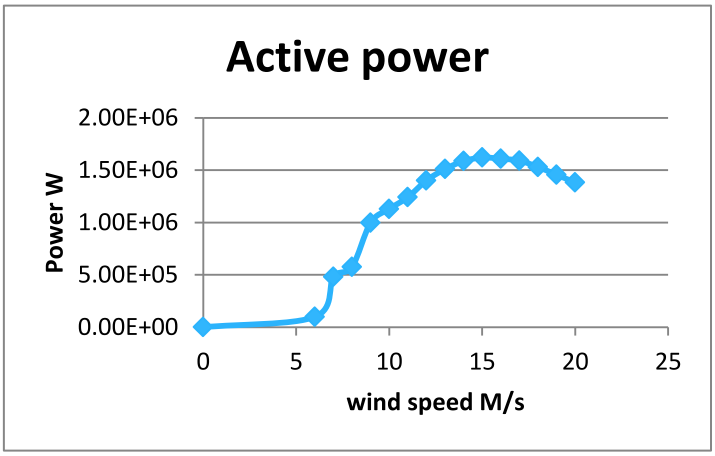

FIGURE 18 POWER CURVE FOR FIXED-SPEED WIND TURBINE

3.2.2 WIND DISTURBANCE

A small wind increase from 10m/s to 15m/s is created to test the model behavior. Characteristics can be found in figure 19. Rotational speed didn't change and other three parameters increased in different ways and to different degrees. The characteristics are the same as the wind turbine in practice.

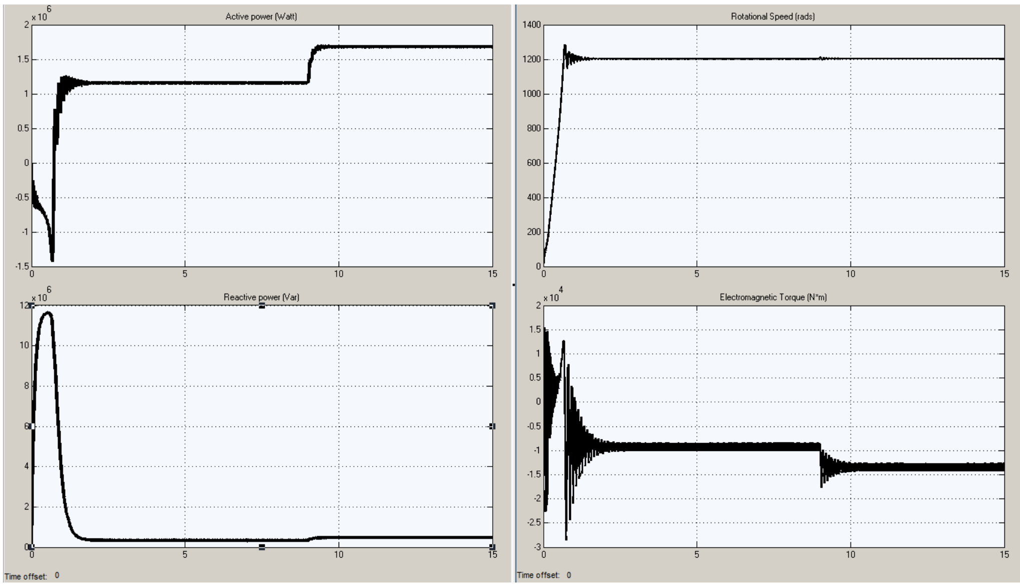

FIGURE 19 FIXED SPEED WIND TURBINE CHARACTERISTICS UNDER WIND DISTURBANCE

3.2.3 VOLTAGE SAG

A three phase fault is made at 9.9 seconds and cleared at 10 seconds (see figure 20). System suffers a fluctuation but finally reach steady-state again. When the fault happened, reactive power consumption increased sharply and then drops to back to steady-state.

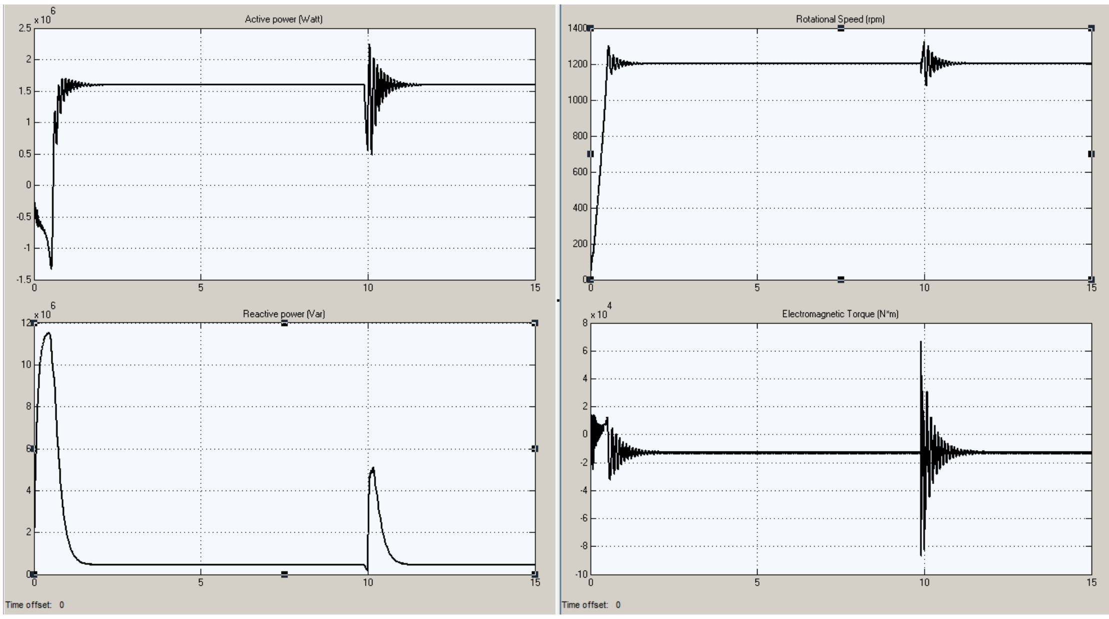

FIGURE 20 THREE PHASE FAULT TIME LENGTH: 0.1 SECOND

Three phase fault is made at 9.85 seconds and cleared at 10 seconds (figure 21). It's clear that, system lost its steady state. Wind turbine should be disconnected from grid until it is ready for reconnection.

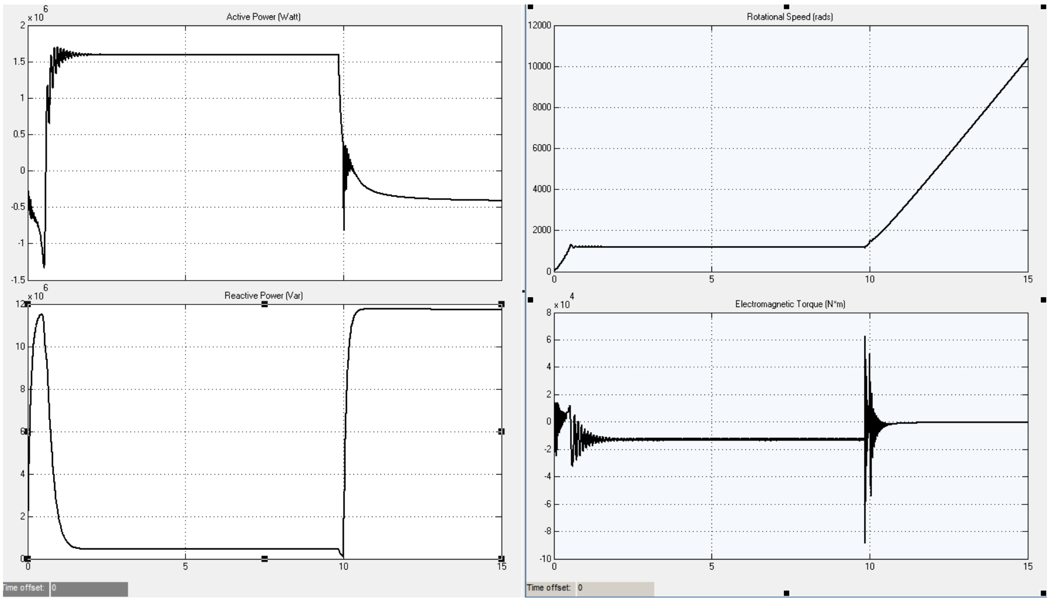

FIGURE 21 THREE PHASE FAULT TIME LENGTH: 0.15 SECONDS

3.3 VARIABLE SLIP WIND TURBINE

Compared with fixed-speed wind turbine, variable slip wind turbine is equipped with an external resistance and a resistance control block. Wound rotor induction machine is employed to make the rotor resistance adjustable.

A controlled voltage source and controlled current source is used to take the place of the variable resistor, detailed model can be seen in figure 22. Since the model is three-phase, so there is one resistor on each phase.

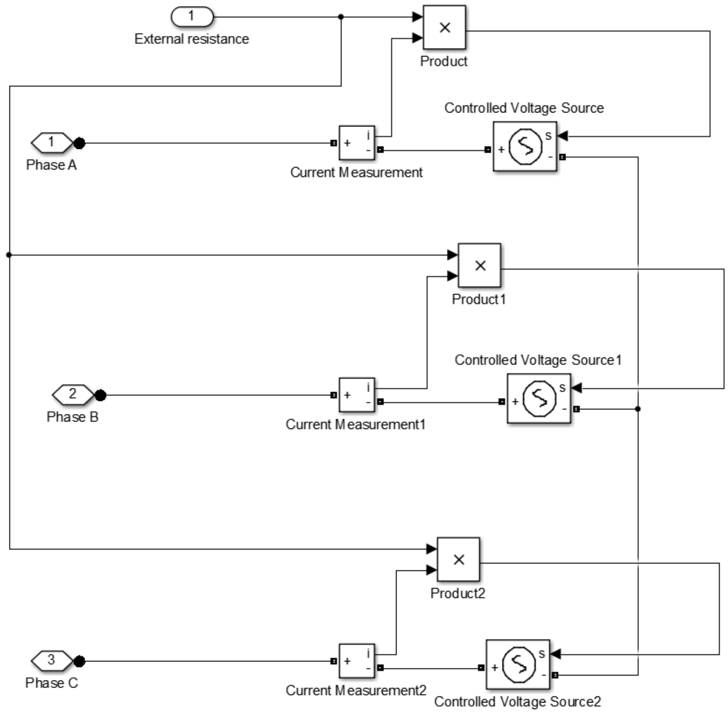

FIGURE 22 MODEL FOR EXTERNAL RESISTANCE

Control system of variable slip wind turbine ensures that the power extracted from the wind at higher than rated wind speed equals to the rated power of the machine. Two PI controllers are applied to generate accurate external resistance signal for generator.

First PI controller is applied to compare the difference between generated power and rated power. Second one aims to compare the current difference and generate external resistance signal. The PI controller detailed model can be seen in figure 23.

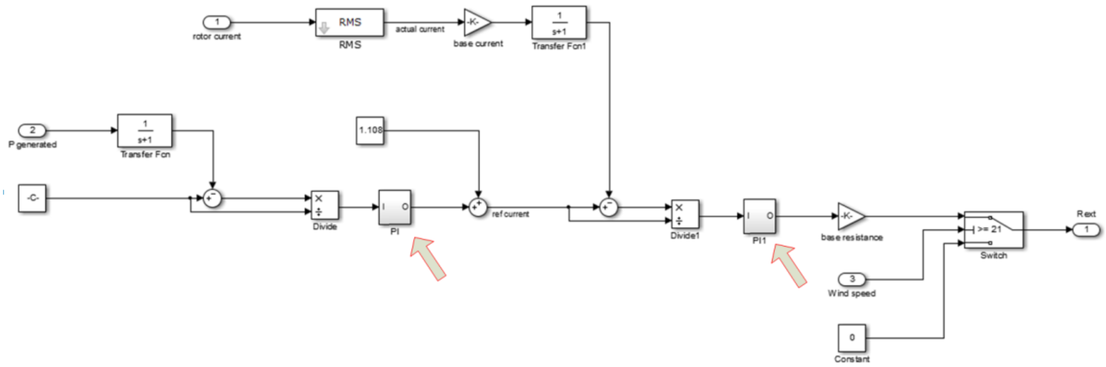

FIGURE 23 VARIABLE SLIP WIND TURBINE CONTROL SYSTEM

After implemented two sections mentioned above, the model for variable slip wind turbine is completed which is shown in figure 24.

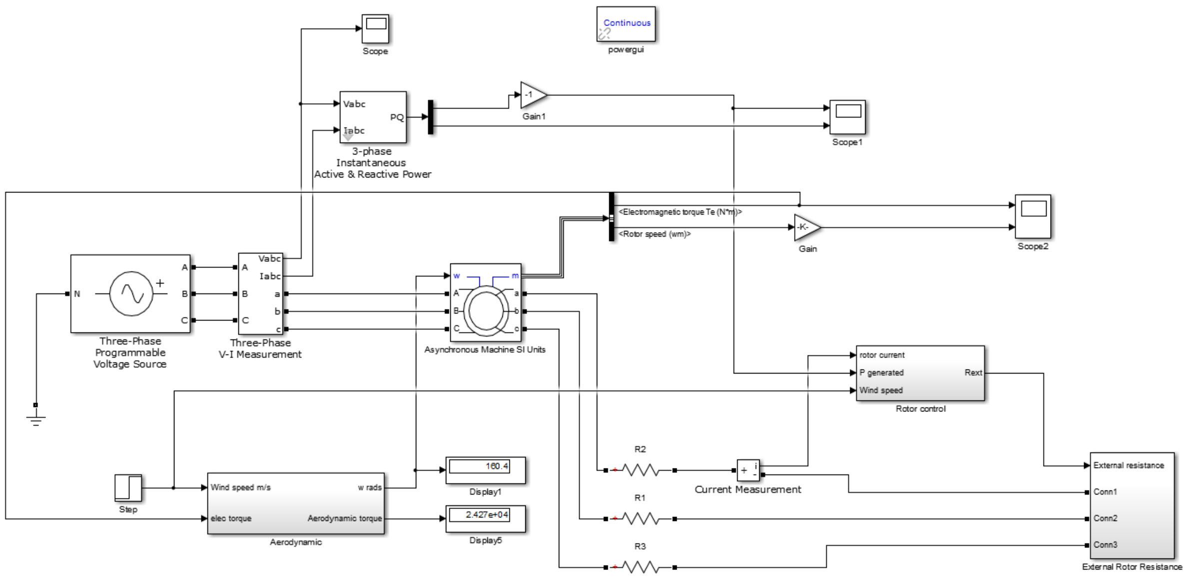

FIGURE 24 VARIABLE SLIP WIND TURBINE COMPLETE MODEL

3.4 VARIABLE SLIP WIND TURBINE VALIDATION

3.4.1 POWER CURVE

Power curve for variable slip wind turbine is shown in figure 25. Before 20m/s, wind speed characteristic is the same as fixed-speed wind turbine. In the region between rated wind speed and cut out wind speed, active power stays at generator rated value.

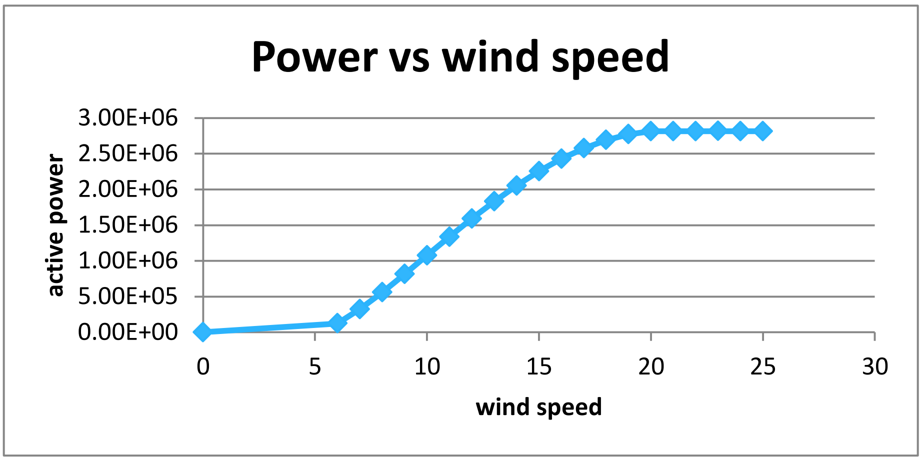

FIGURE 25 VARIABLE SLIP WIND TURBINE POWER CURVE

3.4.2 WIND DISTURBANCE

Wind disturbance is created at 1500s from 21m/s to 23m/s, turbine characteristics can be found in figure 26 and 27.

With a sudden increase of wind speed, PI controller started performing reaction, then external resistance increased which leads to the decrease of active, reactive power, electromechanical torque and rotor speed. After that moment, system returns to a balanced condition gradually under the control of PI controller.

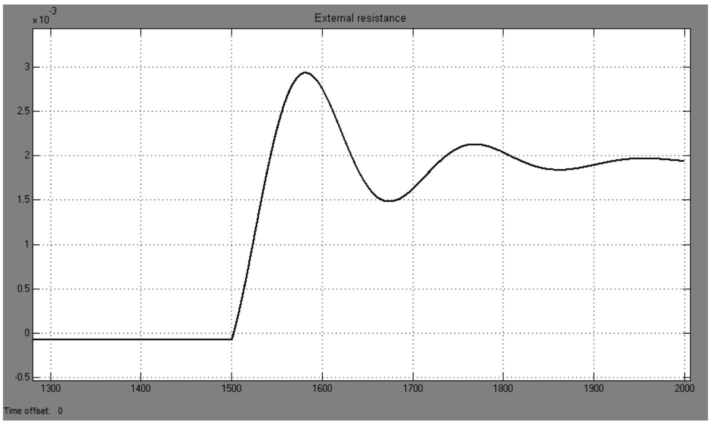

FIGURE 26 VARIABLE SLIP EXTERNAL RESISTANCE UNDER WIND DISTURBANCE

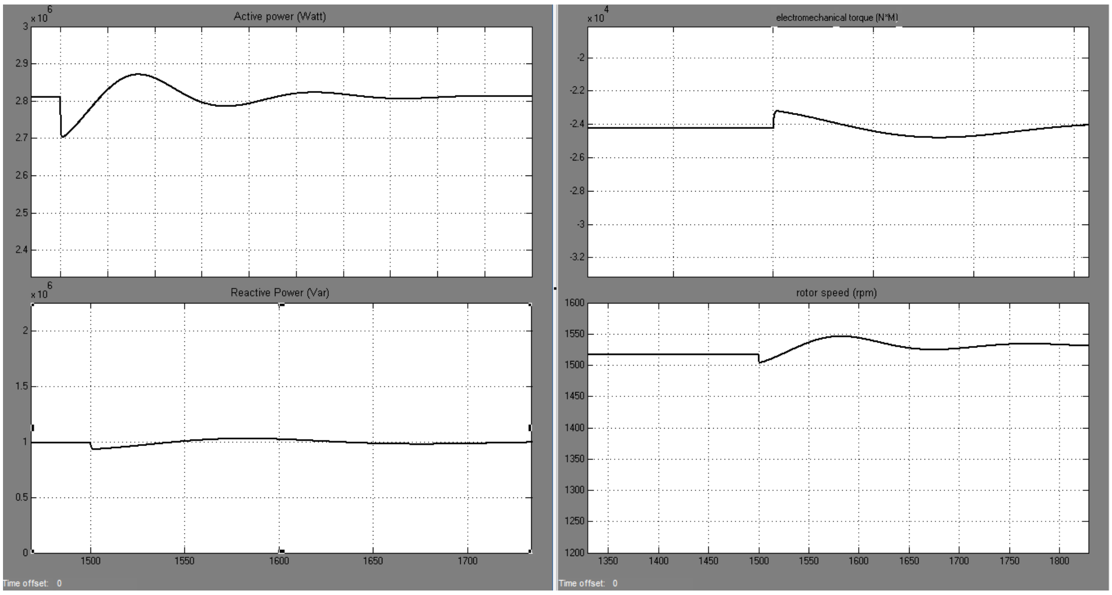

FIGURE 27 VARIABLE SLIP WIND TURBINE CHARACTERISTICS UNDER WIND DISTURBIANCE

3.4.3 VOLTAGE SAG

Voltage sag is created to test the response of wind turbine which exists for 0.3 seconds and the magnitude is reduced by 20%. As shown in figure 28.

Active power, reactive power and torque make immediate response with the change of voltage. At 1500s, three parameters decreased because the decrease of voltage amplitude. After 0.3s, they respond with the sudden increase of voltage amplitude. Rotor speed increased because the lack of electromechanical torque, then it drops back.

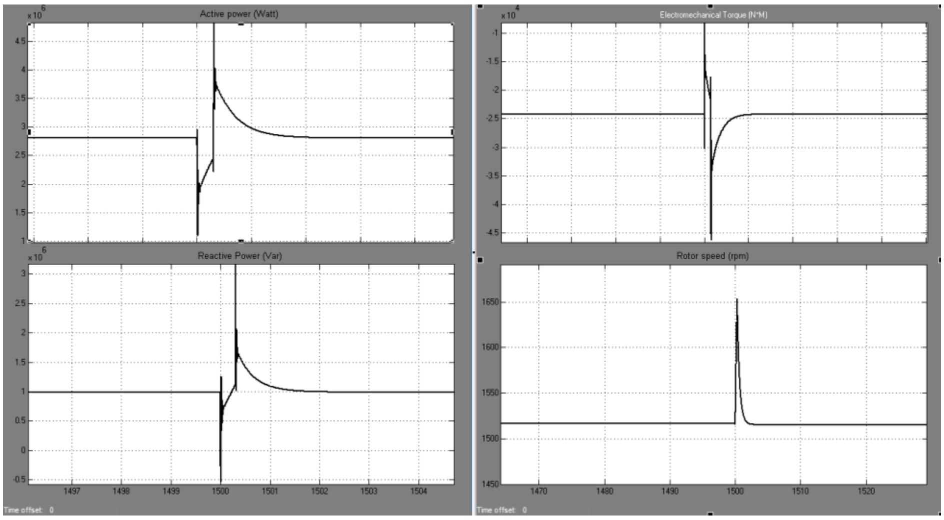

FIGURE 28 TURBINE CHARACTERISTICS UNDER VOLTAGE SAG

3.5 DOUBLY-FED WIND TURBINE SIMPLIFIED MODEL

Wind turbine model uses controlled current sources to represent the behavior of doubly fed induction generator are described in this section. Per-unit mechanical system, active pitch control and per-unit power control are described. The model is built in per-unit system but parameters can be transferred to SI unit easily.

3.5.1 WIND TURBINE MECHANICAL SYSTEM

As we know that the aerodynamic power in the air can be expressed by equation (3-1) (reuk, 2006):

$$P_{wind} = \frac{1}{2}\rho A V_{wind}^3 \tag{3-1}$$

Under rated condition, active power can be expressed as equation (3-2):

$$P_{wind\ rated} = \frac{1}{2}\rho A V_{wind\ rated}^3 \tag{3-2}$$

By converting power into per unit system P_{pu} can be expressed by (3-3)

$$P_{pu} = V_{pu}^3 \tag{3-3}$$

If wind speed is higher than 1.0 p.u. Part of the active power should be removed to keep the system in safe and stable. Extra power can be found using equation (3-4) and (3-5), which is from Mohit (2001).

$$\triangle P = K_{aero}\theta(\theta - \theta_0) \tag{3-4}$$

$$\theta_0 = \frac{\theta_2}{0.75}\left(1 - \frac{1}{V_{wind\ pu}{}^2}\right) \tag{3-5}$$

where:

K_{aero} =0.007

θ = pitch angle of the turbine blades

θ_0 = initial pitch angle

θ_2 = the angle at twice rated wind speed.

“The aerodynamic gain factor K_{aero} has been given a default value of 0.007 determined from the analysis of one set of C_p curves” (WECC, 2006).

The actual aerodynamic power delivered to machine should be equation (3-6).

$$P_{mechanical\ pu} = \mathrm{P}_{pu} - \triangle\ \mathrm{P} = V_{pu}^{3} - K_{aero}\theta(\theta - \theta_0) \quad (3\text{-}6)$$

From single mass inertia equation (3-7) mentioned in 2.3.2:

$$\Gamma_{turbine} - \Gamma_{generator} = J_{equivalent}\frac{d^2\theta(t)}{dt^2} \quad (3\text{-}7)$$

Several conversion procedures are given to equation (3-7).

$$\frac{P_{turbine} - P_{generator}}{\omega} = \Gamma_{turbine} - \Gamma_{generator} = J_{equivalent}\frac{d^2\theta(t)}{dt^2} \quad (3\text{-}8)$$

$$\frac{P_{turbine\ pu} - P_{generator\ pu}}{\omega} = \frac{J_{equivalent}\frac{d^2\theta(t)}{dt^2}}{P_{nom}} \quad (3\text{-}9)$$

$$P_{turbine\ pu} - P_{generator\ pu} = 2 * \frac{1}{2} * \frac{J_{equivalent}\frac{d^2\theta(t)}{dt^2}}{P_{nom}} * \omega \quad (3\text{-}10)$$

From the definition of machine inertia constant (Mohammad, 2006, p. 17)

$$H = \frac{\frac{1}{2}J\omega^2}{P_{nom}} \quad (3\text{-}11)$$

where:

J = inertia

ω = synchronous speed of an induction machine

P = the nominated power of machine

Then, equation (3-7) becomes equation (3-12).

$$P_{turbine\ pu} - P_{generator\ pu} = \frac{2H}{\omega_{sync}}\omega_{pu}\frac{d^2\theta(t)}{dt^2} \quad (3\text{-}12)$$

Rearrange equation (3-12), angular speed difference between generator shaft and generator synchronous speed is shown in equation (3-13):

$$\frac{d\delta}{dt} = \int \frac{(P_{mech\ pu} - P_{elec\ pu})\omega_s}{2H\omega_{pu}} \quad (3\text{-}13)$$

As we know the synchronous speed of generator is (3-14) (E.T.E, 2012).

$$\omega_{sync} = f * \frac{120}{P} \quad (3\text{-}14)$$

Simply add equation (3-13) and (3-14) together. Shaft rotational speed of generator can be found which is shown in equation(3-15):

$$\omega = \omega_s + \frac{d\delta}{dt} \tag{3-15}$$

Mechanical system for doubly-fed induction generator can be found in figure 29.

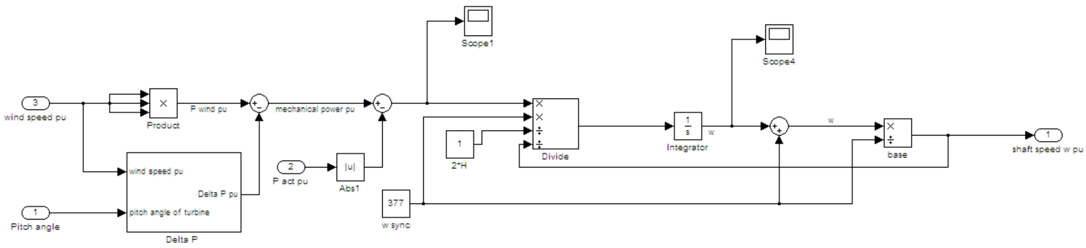

FIGURE 29 MECHANICAL SYSTEM FOR DFIG

3.5.2 PITCH CONTROL

Two PI controllers are employed to produce two control signals which could increase its accuracy. One PI controller is used to compare power signal, and other one is to compare speed signal. Topology can be found in figure 30. PI controller will stop working only if speed difference and power difference is 0. If there are differences exist in the first or the second PI controller, blade pitch angle will be changed to reduce the error.

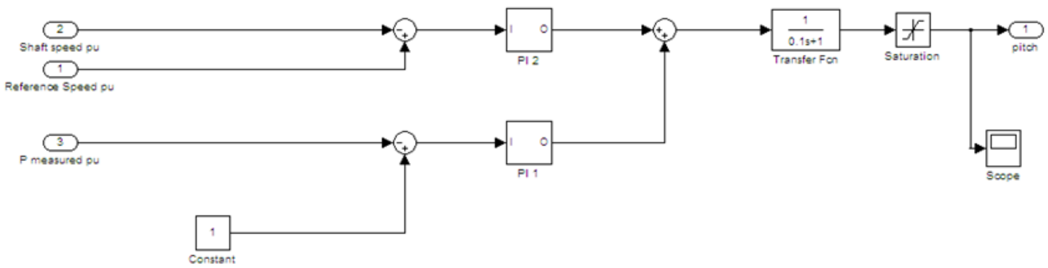

FIGURE 30 ACTIVE PITCH CONTROL SYSTEM

3.5.3 GENERATOR AND POWER CONVERTERS

Generator and converters are realized by using three controlled current sources and several control procedures. To find proper current for each of the controlled current source, PI controlled is applied. As stated in 2.5.2, q-axis current is generated by active power control block and d-axis current is generated by reactive power control block. D-axis direction is the same as the sum of stator flux.

3.5.3.1 ACTIVE POWER CONTROL

Two PI controllers are employed to generated q-axis current. Measured active power is feeding into a look up table (table 2). The table gives the desired rotor speed. Then speed difference will be fed into PI 1. Comparisons between measured active power and reference active power are done by PI 2. The output of PI 2 is regarded as q-axis current. Full schematic diagram is shown in figure 31.

TABLE 2 DESIRED ROTOR SPEED VERSUS MEASURED ACTIVE POWER FROM (MOHIT, 2011)

Active Power	pu	0	0.08	0.16	0.2	0.4	0.6	0.74	0.87	1
Rotor Speed	pu	0.688	0.689	0.69	0.78	0.98	1.12	1.198	1.199	1.2

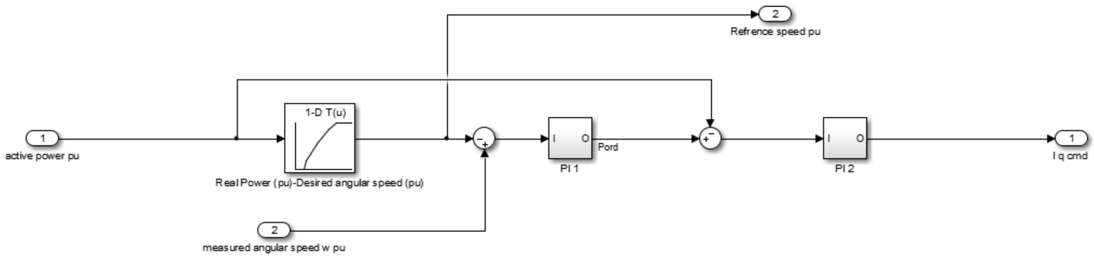

FIGURE 31 ACTIVE POWER CONTROL BLOCK

3.5.3.2 REACTIVE POWER CONTROL

Again, d-axis current is generated by PI controller. Since reference reactive power is defined by user, so simply compare the measured reactive power and required reactive power, d-axis current can be generated by PI controller. Schematic diagram is shown in figure 32:

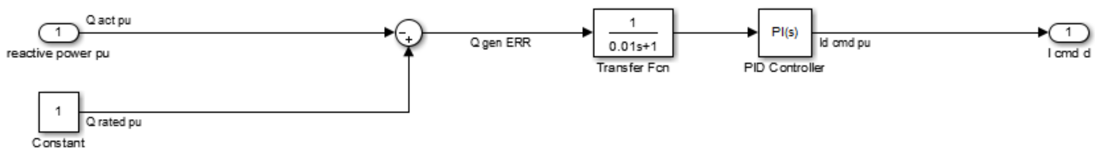

FIGURE 32 REACTIVE POWER CONTROL BLOCK

Connect the blocks described above properly, DFIG simplified model is complete. Full schematic diagram is shown in figure 33.

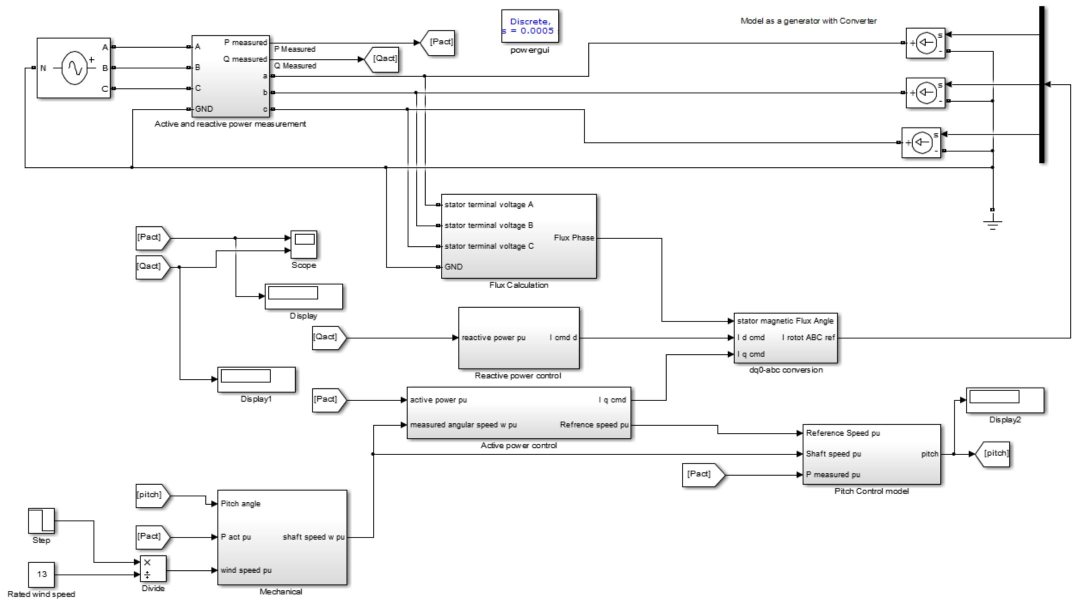

FIGURE 33 DFIG SIMPLIFIED MODEL

3.6 VALIDATION

3.6.1 POWER COMPARISONS

Active power and reactive power in abc reference frame are compared with themselves in dq0 reference frame. The comparison aims to prove the conversion between abc and dq0 reference frame is correct.

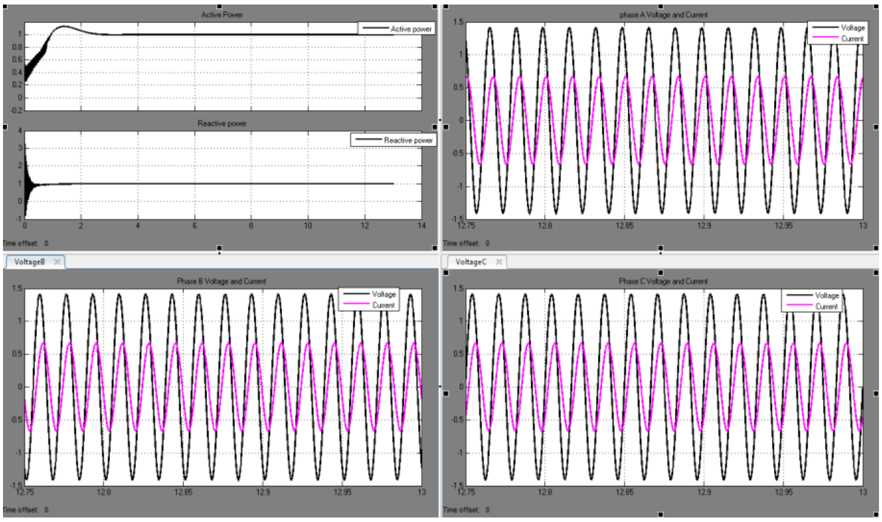

FIGURE 34 THREE PHASE VOLTAGE AND CURRENT WAVEFORMS IN ABC REFERENCE FRAME

From figure 34, maximum voltage is approximately 1.4 per-units. Maximum current is 0.667 per-units. Phase difference measured by Fourier series is 45 degrees approximately. Active power and reactive power is calculated using equation (3-16) and (3-17):

Active power $\mathrm{P} = 3 * V_{rms} * I_{rms} * \cos\alpha = 0.999\mathrm{pu}$ (3-16)

Reactive power $\mathrm{Q} = 3 * V_{rms} * I_{rms} * \sin\alpha = 0.999\mathrm{pu}$ (3-17)

Both the active and reactive power is close to 1 per-unit. Small difference is permitted.

Voltage and current in dq0 reference frame are time invariant under steady-state. The parameters are recorded in table 3.

TABLE 3 VOLTAGE AND CURRENT VALUES IN DQ0 REFERENCE FRAME

	Voltage (per-unit)	Current (per-unit)
d-axis	1.6822	0.4233
q-axis	0.4124	0.7
0-axis	0	0

The active power and reactive power is found by equation (3-18) and (3-19):

$P = (V_d * I_d + V_q * I_q + 2 * V_0 * I_0)$=1.000755p.u. (3-18)

$\mathrm{Q} = (V_q * I_d - V_d * I_q)$=-1.00297p.u. (3-19)

Active and reactive powers are pretty close to 1 per-unit which is expected. And the error is in an acceptable range.

3.6.2 POWER CURVE

The power curve for DFIG simplified model is shown in figure 35. Extracted power follows the extractable power when wind speed is in the range between 6m/s and 13m/s. After 13m/s, extra power is filter out by the angle change of wind turbine.

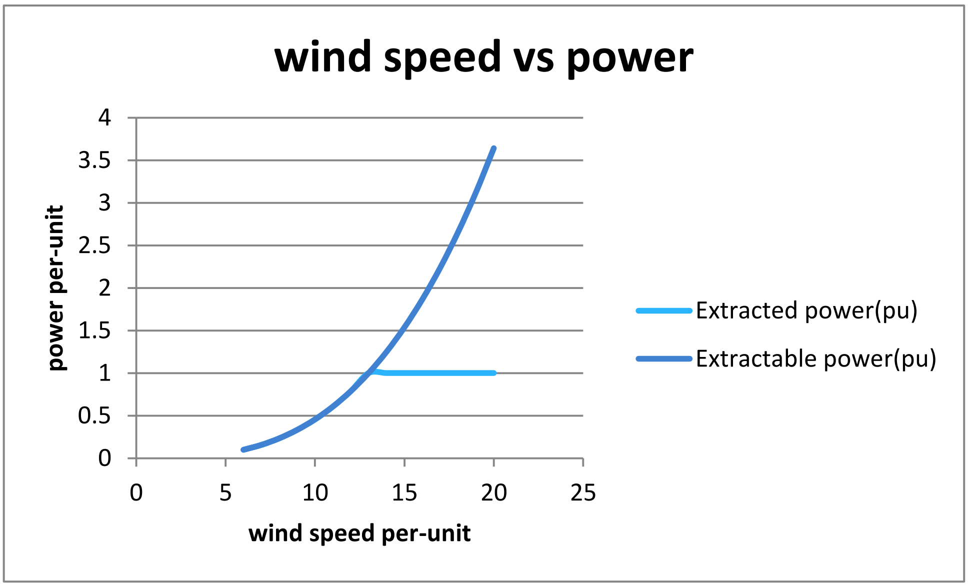

FIGURE 35 EXTRACTABLE POWER VERSUS EXTRACTED POWER

3.6.3 PITCH ANGLE

Blade pitch angel behavior is shown in figure 36. As shown in the figure, when wind speed is below 13m/s, angle stays at 0 degrees, extracted power equals to extractable power which is expected. The pitch angle increases gradually from 13m/s to20m/s. During this range, blade pitch angle increases and it reaches 12 degrees finally. When wind speed is higher than 20m/s, turbine will shut down to prevent further damage.

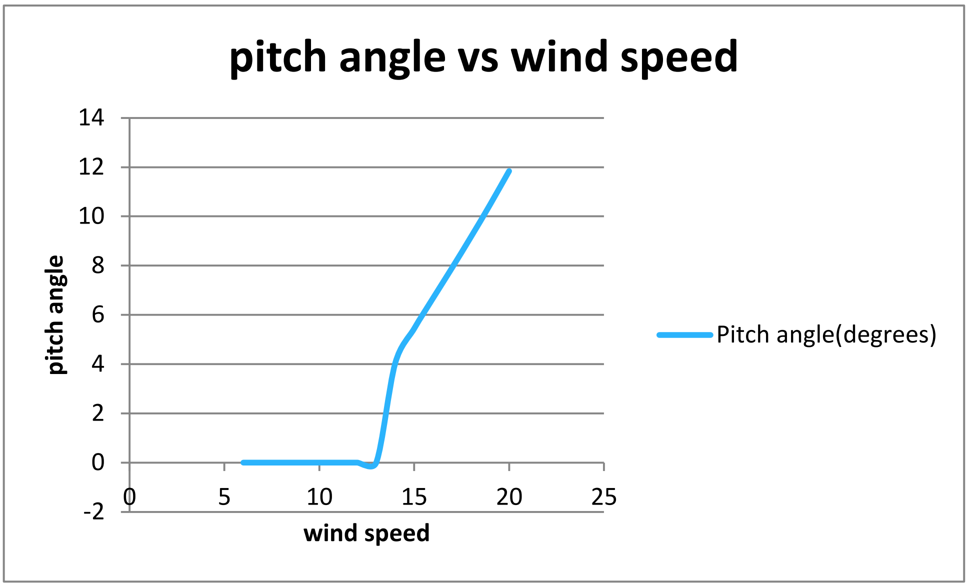

FIGURE 36 PITCH ANGLE VERSUS WIND SPEED

3.6.4 DECOUPLE OF ACTIVE AND REACTIVE POWER

As stated previously, DFIG could decouple the active, reactive power and control them independently. To prove this characteristic, reactive power variation and active power variation is made by keeping the other parameter at constant.

In figure 37, real and reactive power variation for two different conditions is shown. On the left of the figure, active power is changed from 1.0 per-unit to 0.8 per-unit at 7 seconds. System reach 0.8 per-unit at 25 seconds. The reactive power remains unchanged during the change in active power.

On the right side of figure 37, reactive power is changed at 6 seconds instantly, active power didn't change. Small fluctuations can be seen in active power, reason is caused by the simulation step time. The time step is not short enough. But in actual simulation, a shorter step will lead to a long simulation run time. Second reason is the calculation method for stator flux, the method is simplified which had ignored the stator side resistance. But the error is small enough so it can be ignored. The simulation had proved that the active power and reactive power are decoupled.

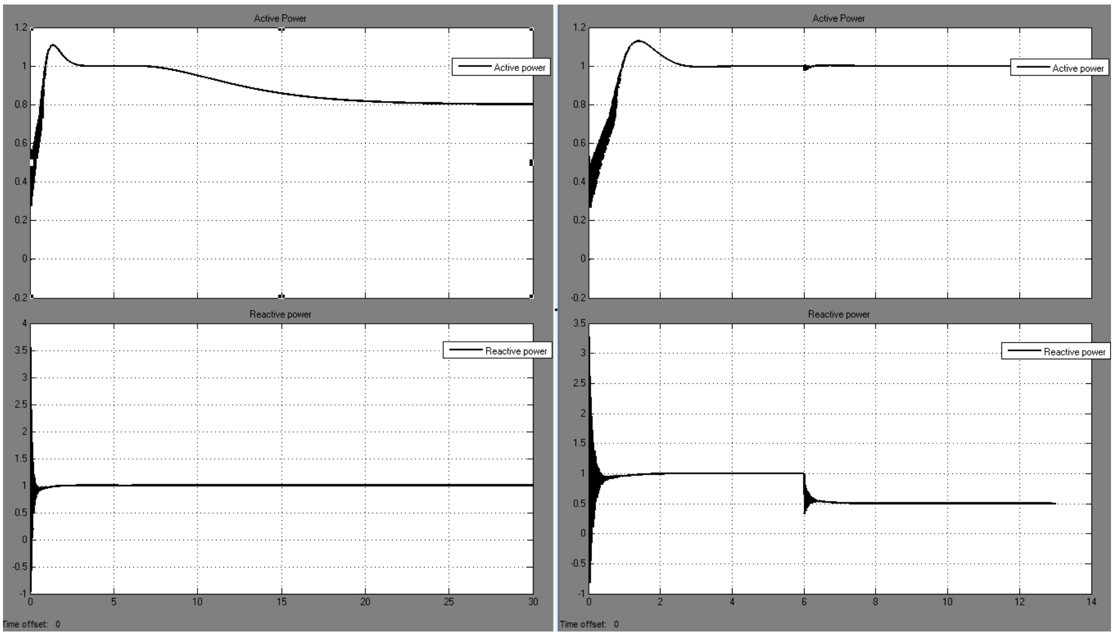

FIGURE 37 ACTIVE AND REACTIVE POWER VARIATION FOR DFIG

3.6.5 WIND DISTURBANCE

Wind disturbance is created to test the behavior of DFIG. Figure 37 shows the power characteristics under wind disturbance. Active power and reactive power are set to 1 per-unit and wind speed is changed. Once the steady state had been reached, an increase or decrease of wind will be made.

As shown in left part of figure 38. Wind speed decrease from 10m/s to 13m/s. The active power dropped to a lower output and reactive power didn't change. Because the wind speed is less than rated wind speed, so the active power is reduced with the extractable power. Reactive power didn't got influenced which is expected.

Similarly, on the right part of figure 38, wind speed increase from 13m/s to 15m/s. Active power suffered a sudden increase and then dropped back to rated value. Reason is the pitch controller had filter out extra power and keeps the generator working at rated output. For reactive power, it remains at constant during simulation as expected.

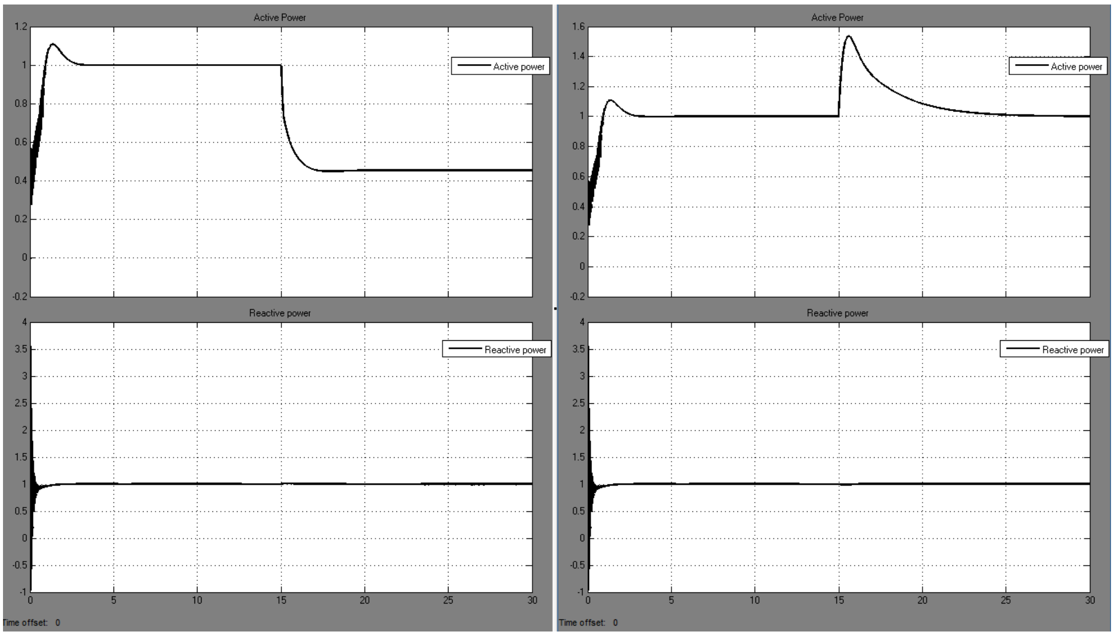

FIGURE 38 ACTIVE AND REACTIVE POWER UNDER WIND DISTURBANCE

3.6.6 VOLTAGE SAG

Wind speed is fixed at rated and voltage sag is created to see the reaction of wind turbine. Voltage sags from 1.0 per-unit to 0.5 per-unit and lasts for 2 seconds. Power characteristics are shown in figure 39.

Both the active and reactive power did immediate response with the voltage variation. At 15 seconds, they drop down because the decrease of voltage. Then at 17 seconds, voltage went back to 1.0 per-unit, both the active and reactive power suffered an increase in magnitude.

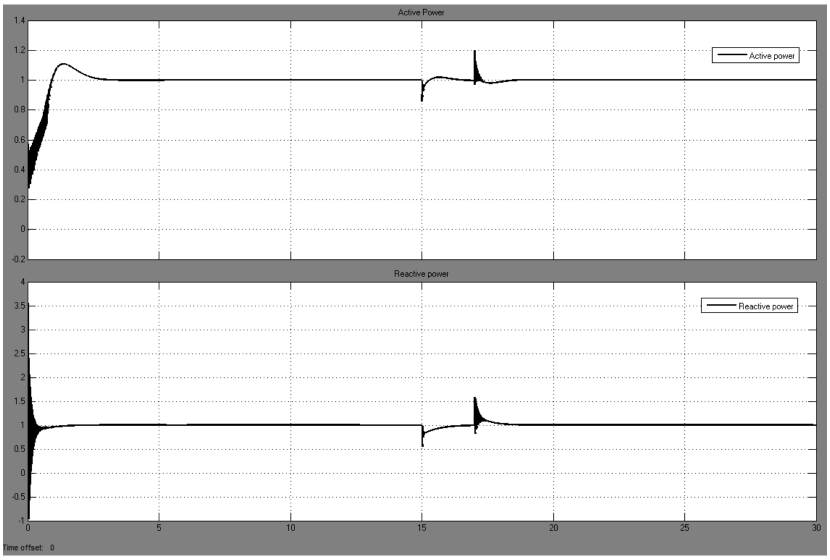

FIGURE 39 VOLTAGE SAG FOR DFIG

Three different wind turbine models are given above with detailed block information and simulation key points. The validation procedures had proved that the models have the ability to reflect basic characteristics of wind turbine. The three wind turbine models are acceptable.

4. SUMMARY AND KEY POINT

Fundamental knowledge part and model construction part are two main parts of this thesis. For the fundamental part, aerodynamic, power control, mechanical system generator and control theory are introduced. Second part includes the detailed blocks structure and complete model for three different types of wind turbines. Different simulations are given to test the behavior of wind turbine. Mathematical equations and related calculation procedures are provided for future research.

Despite from the content mentioned above, some of the key points should be noted:

1. Cp curves are different for different wind turbines. Cp curves and wind turbine should match with each other.
2. Tune of PI controller is important which should be done preciously.
3. If the input signal is higher than the maximum value of a look-up table, Simulink will make prediction based on the trend of the table. Hard saturation should be applied to keep signals within the range.
4. Simulink has several different signal types. It is not permitted to connect different types together.
5. It is important to make every single part work properly before integrating them together. If not, the tune of PI controller will be impossible.

5. CONCLUSION

Basic knowledge and wind turbine working theory had been covered with related mathematical foundations in this report. Wind turbine models and their basic characteristics are also included. Finally, different validations had proved that the model could reflect the basic characteristics of wind turbine in real world. The objective of the work has been met.

Although the models built in this thesis just reflects the basic features of wind turbines and with several shortages. But a reliable dynamic modeling system for wind turbine will be helpful for a variety of problems in future.

6. FUTURE WORK

Due to the time limitation, there are still lots of work which could be done but did not reach. Following the investigation described in this thesis, a number of further investigations can be done.

The models built in this thesis just reflect several basic characteristics of wind turbines, other features can be made based on existed model. Model for DFIG is a simplified one with current source representation. A detailed model with partial frequency converter will be much more helpful. Despite from that, full scale frequency converter wind turbine (Type IV) can be built so that all kinds of wind turbine types will be included.

Different control method can be applied to control the generator of wind turbine. For example the stator flux oriented, rotor flux oriented and air gap flux control can be made. Comparisons of these control methods could be a good topic.

Due to the lack of wind turbine data, comparisons between simulation result and practical result is impossible. If practical data is available in future, comparison between theory result and practical result and make improvement on simulation models can be made.

The models were done by using Simulink. It is possible to adopt the model to other simulation software, such as Power Factory and ICAPS.

7. APPENDIX

FIFTH-ORDER EQUATION FOR INDUCTION GENERATOR

Information for fifth-order equation is from (Mohit, 2011). The equation is derived in a frame which is rotating at a constant speed ω_{ref}. The resulting equations for stator and rotor are:

$$u_s = r_s i_s + \frac{1}{\omega_n}\frac{d\psi_s}{dt} + j\psi_s \frac{\omega_{ref}}{\omega_n}$$

$$u_r = r_r i_r + \frac{1}{\omega_n}\frac{d\psi_r}{dt} + j\psi_r \frac{\omega_{ref-}\omega_g}{\omega_n}$$

$$\psi_s = (x_s + x_m)i_s + x_m i_r$$

$$\psi_r = x_m i_s + (x_m + x_r)i_r$$

Mechanical equation:

$$J\frac{d\omega_g}{dt} = t_{mech} + t_{elec}$$

The electrical torque can be calculated from stator current and flux:

$$t_{elec} = Im(\psi_s + i_s^*)$$

Where:

U_s =voltage

Ψ=flux

I=current

X=reactance

R=resistance

PARK TRANSFORMATION AND CLARKE TRNANSFORMATION

In1929 Robert H. Park introduced a transformation which could transfer three-phase balanced AC values into two-phase DC without losing its characteristics.

Expression of Park transformation (Park, 1929):

$$P = Xdq0 = \frac{2}{3}\begin{bmatrix} cos\theta & \cos(\theta - \frac{2\pi}{3}) & \cos(\theta + \frac{2\pi}{3}) \\ \sin(\theta) & \sin(\theta - \frac{2\pi}{3}) & \sin(\theta + \frac{2\pi}{3}) \\ \frac{1}{2} & \frac{1}{2} & \frac{1}{2} \end{bmatrix} * \begin{bmatrix} X_a \\ X_b \\ X_c \end{bmatrix}$$

X_a, X_b and $X_c$are generic three phase parameters, angle $\theta$is the angle in three phase frame.

Clarke transformation is also called Alpha-Beta transformation. The transformation can be regard as a projection from three-phase parameters to the axis of alpha and beta. The expression of Clarke transformation (W.C. Duesterhoeft, 1951):

$$X_{\alpha\beta\gamma}(t) = \sqrt{\frac{2}{3}}\begin{bmatrix} 1 & -\frac{1}{2} & -\frac{1}{2} \\ 0 & \frac{\sqrt{3}}{2} & -\frac{\sqrt{3}}{2} \\ \frac{1}{2} & \frac{1}{2} & \frac{1}{2} \end{bmatrix} * \begin{bmatrix} X_a \\ X_b \\ X_c \end{bmatrix}$$

Similarly, X_a, X_b and X_c are generic three phase parameters and $X_{\alpha\beta\gamma}$ are parameters in alpha and beta reference frame.

TRANSFORMATION FROM ABC REFERENCE FRAME TO DQ0 REFERENCE FRAME (MOHIT S. , 2011)

The procedure follows (Mohit S. , 2011)

Stationary reference frame:

Stator voltage:

$$V_{as} = r_s i_{as} + \frac{d\lambda_{as}}{dt}$$

$$V_{bs} = r_s i_{bs} + \frac{d\lambda_{bs}}{dt}$$

$$V_{cs} = r_s i_{cs} + \frac{d\lambda_{cs}}{dt}$$

Rotor voltage:

$$V'_{ar} = r'_r i'_{ar} + \frac{d\lambda'_{ar}}{dt}$$

$$V'_{br} = r'_r i'_{br} + \frac{d\lambda'_{br}}{dt}$$

$$V'_{cr} = r'_r i'_{cr} + \frac{d\lambda'_{cr}}{dt}$$

Winding inductance:

$$\overline{L_s} = \begin{bmatrix} L_{ls} + L_{ms} & -\frac{1}{2}L_{ms} & -\frac{1}{2}L_{ms} \\ -\frac{1}{2}L_{ms} & L_{ls} + L_{ms} & -\frac{1}{2}L_{ms} \\ -\frac{1}{2}L_{ms} & -\frac{1}{2}L_{ms} & L_{ls} + L_{ms} \end{bmatrix}$$

$$\overline{L_s} = \begin{bmatrix} L'_{lr} + L_{ms} & -\frac{1}{2}L_{ms} & -\frac{1}{2}L_{ms} \\ -\frac{1}{2}L_{ms} & L'_{lr} + L_{ms} & -\frac{1}{2}L_{ms} \\ -\frac{1}{2}L_{ms} & -\frac{1}{2}L_{ms} & L'_{lr} + L_{ms} \end{bmatrix}$$

$$\overline{L'_{sr}} = L_{ms} \begin{bmatrix} cos\theta_r & cos(\theta_r + 120°) & os(\theta_r - 120°) \\ cos(\theta_r - 120°) & cos\theta_r & cos(\theta_r + 120°) \\ cos(\theta_r + 120°) & os(\theta_r - 120°) & cos\theta_r \end{bmatrix}$$

Flux linkage can be expressed as:

$$\overline{\lambda_{abc\,s}} = \overline{L_s} * \overline{l_{abc\,s}} + \overline{L'_{sr}} * \overline{l'_{abc\,r}}$$

$$\overline{\lambda_{abc\,r}} = \overline{L'_s}^{T} * \overline{l'_{abc\,s}} + \overline{L'_r} * \overline{l'_{abc\,r}}$$

Rearrange above equations we get:

$$V_{abc\,s} = \left(r_s + \frac{d\overline{L_s}}{dt}\right) * \overline{l_{abc\,s}} + \frac{d(\overline{L'_{sr}} * \overline{l'_{abc\,r}})}{dt}$$

$$V'_{abc\,r} = \left(r'_r + \frac{d\overline{L'_r}}{dt}\right) * \overline{i'_{abc\,r}} + \frac{d(\overline{L'_s}^T * \overline{i'_{abc\,s}})}{dt}$$

Using Park Transformation Voltage equation above can be rewrite:

Stator voltage equations:

$$V_{qs} = r_s i_{qs} + \omega\lambda_{ds} + \frac{d\lambda_{qs}}{dt}$$

$$V_{ds} = r_s i_{ds} - \omega\lambda_{qs} + \frac{d\lambda_{ds}}{dt}$$

$$V_{0s} = r_s i_{0s} + \frac{d\lambda_{0s}}{dt}$$

Rotor voltage equations:

$$V'_{qr} = r'_r i'_{qr} + (\omega - \omega_r)\lambda'_{dr} + \frac{d\lambda'_{qs}}{dt}$$

$$V'_{dr} = r'_r i'_{dr} - (\omega - \omega_r)\lambda'_{qr} + \frac{d\lambda'_{ds}}{dt}$$

$$V'_{0r} = r'_r i'_{0r} + \frac{d\lambda'_{0r}}{dt}$$

Same theory applies on flux linkages:

Stator flux equation:

$$\lambda_{qs} = (L_{ls} + L_m)i_{qs} + L_m i'_{qr}$$

$$\lambda_{ds} = (L_{ls} + L_m)i_{ds} + L_m i'_{dr}$$

$$\lambda_{0s} = L_{0s} i_{0s}$$

Rotor Flux Equations:

$$\lambda'_{qr} = L_m i_{qs} + (L'_{lr} + L_m)i'_{qr}$$

$$\lambda'_{dr} = L_m i_{ds} + (L'_{lr} + L_m)i'_{dr}$$

$$\lambda'_{0r} = L'_{lr} i'_{0r}$$

Where:

$$L_M = \frac{3}{2} L_{ms}$$

Reference frame rotates at the speed of ω.

INDUCTION MACHINE TRANSFORMATION FROM ABC TO DQ0

The procedure follows (Mohit Singh, 2011)

Stationary reference frame:

Stator voltage:

$$V_{as} = r_s i_{as} + \frac{d\lambda_{as}}{dt}$$

$$V_{bs} = r_s i_{bs} + \frac{d\lambda_{bs}}{dt}$$

$$V_{cs} = r_s i_{cs} + \frac{d\lambda_{cs}}{dt}$$

Rotor voltage:

$$V'_{ar} = r'_r i'_{ar} + \frac{d\lambda'_{ar}}{dt}$$

$$V'_{br} = r'_r i'_{br} + \frac{d\lambda'_{br}}{dt}$$

$$V'_{cr} = r'_r i'_{cr} + \frac{d\lambda'_{cr}}{dt}$$

Winding inductance:

$$\overline{L_s} = \begin{bmatrix} L_{ls} + L_{ms} & -\frac{1}{2}L_{ms} & -\frac{1}{2}L_{ms} \\ -\frac{1}{2}L_{ms} & L_{ls} + L_{ms} & -\frac{1}{2}L_{ms} \\ -\frac{1}{2}L_{ms} & -\frac{1}{2}L_{ms} & L_{ls} + L_{ms} \end{bmatrix}$$

$$\overline{L_s} = \begin{bmatrix} L'_{lr} + L_{ms} & -\frac{1}{2}L_{ms} & -\frac{1}{2}L_{ms} \\ -\frac{1}{2}L_{ms} & L'_{lr} + L_{ms} & -\frac{1}{2}L_{ms} \\ -\frac{1}{2}L_{ms} & -\frac{1}{2}L_{ms} & L'_{lr} + L_{ms} \end{bmatrix}$$

$$\overline{L'_{sr}} = L_{ms}\begin{bmatrix} cos\theta_r & cos(\theta_r + 120°) & os(\theta_r - 120°) \\ cos(\theta_r - 120°) & cos\theta_r & cos(\theta_r + 120°) \\ cos(\theta_r + 120°) & os(\theta_r - 120°) & cos\theta_r \end{bmatrix}$$

Flux linkage can be expressed as:

$$\overline{\lambda_{abc\,s}} = \overline{L_s} * \overline{l_{abc\,s}} + \overline{L'_{sr}} * \overline{l'_{abc\,r}}$$

$$\overline{\lambda_{abc\,r}} = \overline{L'_s}^T * \overline{l'_{abc\,s}} + \overline{L'_r} * \overline{l'_{abc\,r}}$$

Rearrange above equations we get:

$$V_{abc\,s} = \left(r_s + \frac{d\overline{L_s}}{dt}\right) * \overline{l_{abc\,s}} + \frac{d(\overline{L'_{sr}} * \overline{l'_{abc\,r}})}{dt}$$

$$V'_{abc\,r} = \left(r'_r + \frac{d\overline{L'_r}}{dt}\right) * \overline{l'_{abc\,r}} + \frac{d(\overline{L'_s}^T * \overline{l'_{abc\,s}})}{dt}$$

Using Park Transformation Voltage equation above can be rewrite:

Stator voltage equations:

$$V_{qs} = r_s i_{qs} + \omega\lambda_{ds} + \frac{d\lambda_{qs}}{dt}$$

$$V_{ds} = r_s i_{ds} - \omega\lambda_{qs} + \frac{d\lambda_{ds}}{dt}$$

$$V_{0s} = r_s i_{0s} + \frac{d\lambda_{0s}}{dt}$$

Rotor voltage equations:

$$V'_{qr} = r'_r i'_{qr} + (\omega - \omega_r)\lambda'_{dr} + \frac{d\lambda'_{qs}}{dt}$$

$$V'_{dr} = r'_r i'_{dr} - (\omega - \omega_r)\lambda'_{qr} + \frac{d\lambda'_{ds}}{dt}$$

$$V'_{0r} = r'_r i'_{0r} + \frac{d\lambda'_{0r}}{dt}$$

Same theory applies on flux linkages:

Stator flux equation:

$$\lambda_{qs} = (L_{ls} + L_m)i_{qs} + L_m i'_{qr}$$

$$\lambda_{ds} = (L_{ls} + L_m)i_{ds} + L_m i'_{dr}$$

$$\lambda_{0s} = L_{0s} i_{0s}$$

Rotor Flux Equations:

$$\lambda'_{qr} = L_m i_{qs} + (L'_{lr} + L_m)i'_{qr}$$

$$\lambda'_{dr} = L_m i_{ds} + (L'_{lr} + L_m)i'_{dr}$$

$$\lambda'_{0r} = L'_{lr} i'_{0r}$$

Where:

$$L_M = \frac{3}{2} L_{ms}$$

Reference frame rotates at the speed of ω.

POWER CURVES

POWER CURVE TABLE FOR FIXED SPEED WIND TURBINE

TABLE 4 POWER CURVE FOR FIXED SPEED WIND TURBINE

Wind speed m/s	Active power W
0	0
6	99290
7	480800
8	574700
9	998200
10	1129000
11	1242000
12	1401000
13	1510000
14	1587000
15	1620000
16	1610000
17	1590000
18	1531000

19	1456000
20	1383000

POWER CURVES FOR VARIABLE SLIP WIND TURBINE

TABLE 5 POWER CURVE FOR VARIABLE SLIP WIND TURBINE

Wind speed	Rotor speed/RPM	Active power	Slip	External resistance
0	NA	0	NA	NA
6	1214	1.23E+05	-0.0116667	0
7	1237	3.24E+05	-0.0308333	0
8	1263	5.58E+05	-0.0525	0
9	1291	8.13E+05	-0.0758333	0
10	1320	1.08E+06	-0.1	0
11	1349	1.34E+06	-0.1241667	0
12	1377	1.59E+06	-0.1475	0
13	1404	1.83E+06	-0.17	0
14	1429	2.05E+06	-0.1908333	0
15	1452	2.25E+06	-0.21	0
16	1472	2.43E+06	-0.2266667	0
17	1489	2.58E+06	-0.2408333	0
18	1503	2.69E+06	-0.2525	0
19	1512	2.77E+06	-0.26	0
20	1517	2.81E+06	-0.2641667	0
21	1518	2.81E+06	-0.265	0
22	1522	2.81E+06	-0.2683333	0.0006797
23	1531	2.82E+06	-0.2758333	0.001937
24	1543	2.81E+06	-0.2858333	0.003526
25	1556	2.81E+06	-0.2966667	0.005367

POWER CURVE FOR VALIDATION DFIG (SIMPLIFIED)

Wind Speed(m/s)	Extracted power(pu)	Extractable power(pu)	Reactive power(pu)	Pitch angle(degrees)
6	0.0985	0.098315885	1	0
7	0.1553	0.156121985	1	0
8	0.2326	0.233045061	1	0
9	0.3318	0.331816113	1	0
10	0.455	0.455166136	1	0
11	0.6055	0.605826127	1	0
12	0.7866	0.786527082	1	0
13	1	1	1	0
14	1	1.248975876	1	-4.034
15	1	1.536185708	1	-5.443
16	1	1.864360492	1	-6.686
17	1	2.236231224	1	-7.916
18	1	2.654528903	1	-9.176
19	1	3.121984524	1	-10.48
20	1	3.641329085	1	-11.84

WIND TURBINE SIMULATION PARAMETERS.

FIXED SPEED WIND TURBINE

Case 1		
Fixed speed wind turbine		
Regulation Method	Active Stall	
Rotor Diameter	72	m
Hub Height	62/78	m
Number of Blades	3	
Cut-in Wind Speed	4	m/s
Cut-out Wind Speed	20	m/s
Rated Wind Speed	15	m/s
Rotor Speed	17.3	rpm
Turns Ratio	65	

Generator Ratings

Rated Power	1.50E+06	VA
Rated Voltage	690	V line to line
Number of Poles	6	
Rated Frequency	60	HZ

Generator Parameters

Stator Winding Resistance	0.0047	pu
Stator Winding Inductance	0.08	pu
Rotor Resistance	0.0021	pu
Rotor Inductance	0.0478	pu
Mutual Inductance	6.8	pu
Angular moment of inertia	0.578	s

VARIABLE SPEED WIND TURBINE

Case 2		
Variable slip wind turbine		
Regulation Method	Active Stall	
Rotor Diameter	63	m
Hub Height	64	m
Number of Blades	3	
Cut-in Wind Speed	6	m/s
Cut-out Wind Speed	25	m/s
Rated Wind Speed	21	m/s
Rotor Speed	variable	rpm

Generator Ratings

Rated Power	2.50E+06	VA
Rated Voltage	690	V line to line
Number of Poles	6	
Rated Frequency	60	HZ

Generator Parameters

Stator Winding Resistance	0.005	pu
Rotor Resistance(outside)	0.0021	pu
Stator Winding Inductance	0.08	pu
Rotor Resistance(inside)	1.00E-06	pu
Rotor Inductance	0.0478	pu
Mutual Inductance	6.8	pu
Angular moment of inertia	0.578	s

TABLE OF FIGURE

BIBLIOGRAPHY

Albert, B. (1926). Wind Energy and its Use by Windmills.

B.Hopfensperger, D. a. (2000). Stator-f lux-oriented control of a doubly-fed induction. 243.

council, G. w. (2012). *Global wind report Annual Market Update 2012.*

E.T.E. (2012). *Elec-toolbox*. Retrieved 2014, from http://www.elec-toolbox.com/Formulas/Motor/mtrform.htm

Florin, I. (2004). *Wind Turbine Blockset in Matlab/Simulink.* Alaborg University.

G. Ramtharan, O. A.-L. (2006). *Influence of structural dynamic representations of FSIG wind.*

Hansen. (2007). *Generator and power electronics for wind turbine .* John Wiley and Sons.

Machowiski, J. W. (2008). Power System Dynamics Stability and Control. In J. Machowski. hohn Wiley & Sons,Ltd.

Mohammad, A. M. (2006). Synchronous Machine Dynamics. Perth, WA, Australia.

Mohit. (2011). Dynamic models for wind turbines nad wid power plants. *NREL*.

Mohit, S. (2011). *Dynamic models for wind turbines and Wind power Plants.* Austin: NERL.

Nathan, D. (2004). *Gear Ratios and Mechanical Advantage*. Retrieved 2013, from MAELABS: http://maelabs.ucsd.edu/mae_guides/machine_design/machine_design_basics/Mech_Ad/mech_ad.htm

Okedu, K. E. (2012). *Effects of Drive Train Model Parameters on a Variable Speed Wind Turbine.* Kitami Institute of Technology, Department of Electrical and Electronic Engineering,, Hokkaido, Japan.

O'Kelly, D. (1991). *Performance and control of electrical machines.* McGraw-Hill.

Park, R. (1929). Two reaction THeory of Synchronous Machines. *AIEE*.

Platt, A. (2012). *NWTC Design Codes (WT_Perf by Andrew Platt).* Retrieved from http://wind.nrel.gov/designcodes/simulators/wtperf/. Last modified 26-November-2012; accessed 26-November-2012

Prof. Zoran Vukic, P. (2002). lecture on pid controller. USA.

Ragheb, & M., M. R. (2011). Wind Turbines Theory - The Betz equation and optimal Tip speed ratio. In R. Carriveau, *Fundamemtal and advance topics in wind power.* Intech China/Intech Europe.

Ramtharan, G., & Olimpo Anaya-Lara, E. B. (2006). *Influence of structural dynamic representations of FSIG wind.*

reuk. (2006). *Calculation of wind Power*. Retrieved 2014, from REUK: http://www.reuk.co.uk/Calculation-of-Wind-Power.htm

Robert, J. H. (2009). *Sustainability in Energy and Buildings.* Springer.

Royal, a. o. (2014). *Wind Turbine Power Calculation.*

Smith, C. a. (1976). Dynamics of wind generator on electric utility networks. In IEEE, *Transactions on Aerospace and Electronic System* (pp. 483-493).

W.C. Duesterhoeft, M. W. (1951, July). Determination of Instantaneous Current and Voltage by means of Alpha, Beta and Zero Component. *Transactions of the American Institite of enectrical engineering*.

WECC. (2006). *Generic typr-3 wind turbine-generator model for grid studies.*

Wiki. (2014). *PID COntroller*. Retrieved 2014, from Wikipedia: http://en.wikipedia.org/wiki/PID_controller